MATERIALS ENGINEERING

KEYWORDS: *beryllium, stainless steel, heat conductance*

EXPERIMENTAL MEASUREMENT OF THE INTERFACE HEAT CONDUCTANCE BETWEEN NONCONFORMING BERYLLIUM AND TYPE 316 STAINLESS STEEL SURFACES SUBJECTED TO NONUNIFORM THERMAL DEFORMATIONS

ROBERT DEAN ABELSON and MOHAMED A. ABDOU*
University of California, Los Angeles
Mechanical and Aerospace Engineering Department
43-133 Engineering IV, Box 951597, Los Angeles, California 90095-1597

Received February 7, 2000
Accepted for Publication August 8, 2000

In fusion blanket designs that employ beryllium as a neutron multiplier, the interface conductance h plays a key role in evaluating the blanket's thermal profile. Therefore, an extensive experimental program was conducted to measure the magnitude of h between nonconforming beryllium and Type 316 stainless steel surfaces subjected to nonuniform thermal deformations. The magnitude of h was measured as a function of relevant environmental, surface, and geometric parameters, including surface roughness, contact pressure, gas pressure, gas type, and magnitude and direction of heat flow. The results indicate the following: (a) Decreasing the interfacial surface roughness from 6.28 to 0.28 μm, in 760 Torr of helium, increased the magnitude of h by up to 100%; however, increasing the surface roughness reduced the dependence of h on the magnitude of the contact pressure. (b) The interface conductance was significantly higher for measurements made in helium gas as opposed to air. Additionally, the sensitivity of h to the gas pressure was significantly greater for runs conducted in helium and/or with smoother surfaces. This sensitivity was reduced in air and/or with roughened surfaces, and it was essentially nonexistent for the 6.25-μm specimen for air pressures exceeding 76 Torr. (c) For runs conducted in vacuum, the interface conductance was more sensitive to heat flux than when runs were conducted in 760 Torr of helium. (d) The interface conductance was found to be dependent on the direction of heat flux. When the specimens were arranged so that heat flowed from the steel to the beryllium disk, the magnitude of h was generally greater than in the opposite direction.

I. INTRODUCTION

When an interface is composed of two perfectly smooth, flat and clean surfaces, the laws of thermodynamics tell us that each of the two surfaces must be at the same temperature and the interfacial resistance is nil. In reality, however, engineering surfaces are likely to be roughened, partially oxidized, contaminated with dirt, etc. Because of gaps in the interface, these surfaces typically make contact over <5% of their total area, with conduction being highly three-dimensional near the interface region. In addition to contact conduction, there may also be parallel paths of conduction across the gaps (via an interstitial fluid) or by radiation. Figure 1 shows the temperature distribution across two layers of a composite wall separated by an interface formed from two roughened surfaces.

*E-mail: abdou@fusion.ucla.edu

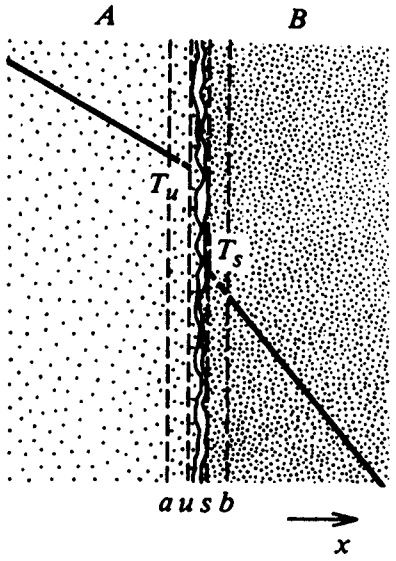

Fig. 1. Temperature distribution near a real surface.[1]

To understand the interface conductance phenomenon, we define two mathematical surfaces, the *u*- and *s*-surfaces, located infinitely close to and on either side of the real interface. The *a*- and *b*-surfaces are defined to be just far enough from the interface such that heat conduction is one-dimensional. Because of three-dimensional effects, there is no unique temperature profile between the *a*- and *b*-surfaces. Instead, the temperature distribution at the *u*- and *s*-surfaces is extrapolated from the bulk material to the interface. For real surfaces, there will be a discontinuity of temperature across the interface, $(T_u \neq T_s)$.

The thermal resistance to heat flow across the interface is called the interface resistance, but one often uses the reciprocal of this quantity, known as the interface conductance, *h*, in everyday engineering work. The definition of the interface conductance is as follows:

$$h \equiv \frac{q}{T_u - T_s} = \frac{q}{\Delta T_i} \quad . \tag{1}$$

Generally, *h* is a complicated function of a multitude of parameters including contact pressure, gas pressure, heat flux, and various surface and material properties. In cases where both contacting surfaces are composed of the same material, the effects of differential thermal expansion will generally have little effect on the value of *h*. These surfaces are said to be "conforming" in that they remain flush against one another at all times. However, in cases where the two surfaces are composed of widely differing thermomechanical properties (i.e., beryllium and stainless steel), there exists the possibility that one surface will thermally deform to a greater extent than the other, resulting in gaps developing within the interface. Since gaps of only a few microns in size can significantly degrade interfacial heat transfer, the need to accurately measure and predict the interface heat conductance is of vital concern.

Of great interest is the dependence of the interface conductance on the magnitude of the heat flux. Increasing the heat flux is expected to create interstitial gaps (due to nonconforming thermal expansion), which can significantly degrade the value of *h*. This is of concern in such high-heat flux systems as cooling units for hypersonic aircraft, supercomputers, and nuclear fuel assemblies. Of more recent concern, however, is the design of tritium-breeding blankets for the first generation of fusion reactors. Because these breeder blankets must be operated within a narrow temperature window to maximize tritium extraction and minimize radiation damage, the need to predict the thermal profile throughout the blanket volume is a critical design issue. In one design,[2] the breeder blanket is constructed from numerous blocks of beryllium mated against an adjacent steel structure. Because the heat transfer between the beryllium and the steel structure is dependent on the interfacial conductance between the two surfaces, it is clear that the engineer must have realistic estimates of the magnitude and sensitivity of *h* to numerous environmental parameters before the blanket design can be optimized.

To obtain these interface conductance data, an experimental program has been developed to measure *h* for an interface composed of solid beryllium and Type 316 stainless steel. Measurements of interface heat conductance were made as a function of gas pressure, gas composition, surface roughness, and contact load. Additionally, to measure the sensitivity of *h* to the effects of thermally induced differential expansions, the direction and magnitude of the heat flux was varied, as was the diameter of the specimens.

Analysis of the heat transfer across an interface identifies three modes of heat transport:

1. conduction across the points of surface-surface contact
2. conduction across the interstitial gas layer
3. radiative heat transport.

Typically, the radiative component is small for most applications and thus will not be considered here. For measurements made in vacuum, the interfacial heat transport is limited to heat conduction across the area of beryllium-Type 316 stainless steel contact. For runs conducted in gas, heat transport across the beryllium-Type 316 stainless steel interface is via conduction across points of surface-surface contact, as well as across the interstitial gas layer. In the literature, the aforementioned two modes of interfacial heat transfer are often referred to as the *contact conductance*, h_c, and the *gas conductance*, h_g. The total interface conductance is expressed as the sum of these two components:

$$h = h_c + h_g \quad .$$

The thermal conductivity of gas is typically several orders of magnitude less than the thermal conductivity of the surface asperities of metal surfaces. However, because the diameter of the surface asperities is very small (on the order of tenths of microns) and the ratio of the contact area to the total surface area is <5%, the thermal resistance of the surface asperities is often much greater than the thermal resistance of the interstitial gas layer. The significance of this is that the value of h_g can be orders of magnitude greater than the value of h_c for runs conducted at high pressures (760 Torr) and with a high-thermal-conductivity gas (helium).

Examination of interface conductance theory and the experimental literature identifies two phenomena that determine how the magnitude of h varies with respect to the interfacial heat flux. The first phenomenon is nonconforming thermal expansion of the test specimens. Raising the heat flux increases the amount of thermal expansion experienced by the beryllium and steel specimens. As will be seen later in this paper, the degree of this thermal expansion is directly related to the coefficient of thermal expansion α and the inverse of the thermal conductivity k^{-1} of the test specimens. Steel has larger values of α and k^{-1} with respect to beryllium, and thus, steel thermally deflects to a greater extent than does beryllium. This results in the formation of interstitial gaps between the two surfaces. The geometry of the deflection profile is dependent on the direction of heat flow with respect to the position of the beryllium and Type 316 stainless steel specimens. When heat flows from the steel to the beryllium surface (abbreviated SaB), the disk-deflection profile is expected to be that of Fig. 2a. The contact area for disks in the SaB configuration is an annular region about the outer perimeter of the specimens. When heat flows from the beryllium to the steel disk (abbreviated as BaS), the disk deflection profile is expected to be that of Fig. 2b. The contact area in the BaS configuration is a concentrically located circular region, whose diameter is a function of the surface roughness

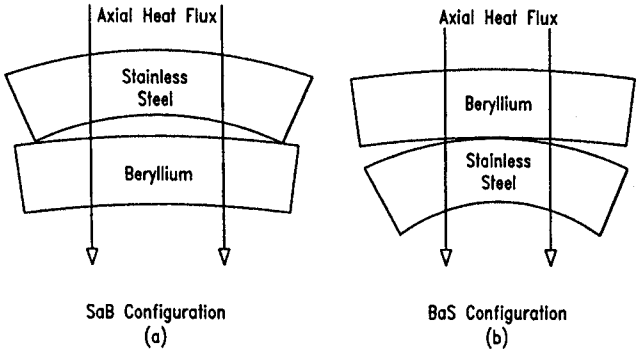

Fig. 2. Two configurations of thermal deformation for the beryllium and stainless steel disks (profiles are highly exaggerated for clarity).

of the test specimens and the magnitude of the heat flux. As the value of q is raised, the gap between the beryllium and the Type 316 stainless steel disks grows larger, decreasing the amount of contact area between the two surfaces (reducing the value of h_c) and increases the mean separation distance between the two surfaces (reducing the value of h_g). Thus, one would expect that raising the heat flux would always lower the magnitude of the interface conductance. There is, however, another simultaneously occurring phenomenon that acts to increase the value of h.

Based on interface conductance theory, the magnitude of the interface conductance is directly related to the thermal conductivity of the test specimens k_s, and the thermal conductivity of the interstitial gas k_g. When the magnitude of the heat flux is increased, the mean interface temperature also increased.[3] Since the thermal conductivity of steel and all gases increases with temperature, one might expect that h would increase with heat flux were it not for the deleterious effects of nonconforming thermal expansion.

Additionally, the literature indicates that the strength S_y and the Young's modulus E of steel and beryllium decrease with increasing temperature. When a load is applied to the beryllium-Type 316 stainless steel specimens, the magnitude of S_y and E determines how much microscopic deformation (of the asperity peaks) and how much macroscopic bending (of the disk structure) occurs as a result of the applied load. As the heat flux is raised and the mean interface temperature increased, the value of S_y and E are both reduced. This results in greater deformation of the surface peaks, allowing the two surfaces to more closely approach one another. This raises the value of the contact conductance h_c (via an increased amount of surface-contact area), as well as raising the value of the gas conductance h_g (by decreasing the mean separation distance between the steel and beryllium surfaces). Furthermore, specimens at higher temperatures are more susceptible to macroscopic bending (i.e., both disks tend to flatten against each other) for a given value of contact pressure due to the degraded values of material strength and Young's modulus at elevated temperatures. As before, this macroscopic deflection acts to increase the surface-contact area and reduce the mean separation distance between the Type 316 stainless steel and beryllium surfaces, resulting in an enhancement in the magnitude of h with increasing heat flux. Thus, increasing the interfacial heat flux should raise the value of h if it were not for the presence of nonuniform thermal expansion.

The question of which of the two aforementioned phenomena dominates the value of h is extremely complex, as it is a function of the surface roughness, mean asperity slope, average interface temperature, gas pressure, and type of gas used. The ability to predict whether the interface conductance will increase or decrease with heat flux is not a trivial task, and no model currently exists that can accurately evaluate the dependence of h_c and h_g

on the value of q. Thus, one must rely on experimental measurements of h to obtain an understanding of the sensitivity of interface conductance upon the magnitude of the heat flux.

To obtain accurate h measurements, considerable care was taken in designing the interface conductance test apparatus. Eleven individual error sources (thermocouple calibration errors, lengths between thermocouples, radiation and convection losses, etc.) were explicitly accounted for in calculating the expected accuracy of the interface conductance measurements. Furthermore, two individual sensitivity analyses were performed to determine the expected accuracy of the test rig when: (a) all error sources are treated as random errors and (b) the random errors and bias errors are treated individually. In addition, because the existing thermal conductivity data in the literature were found to be a major source of error in measuring h, two additional test rigs were designed and constructed to measure the thermal conductivity of the steel specimen and an aluminum flux meter. Because of the relatively high thermal conductivity of beryllium, the error introduced by using the data available in the literature is small enough ($\delta h < 2\%$) not to warrant the building of a fourth test rig.

In summary, past research has found that gaps as small as a few microns can drastically reduce the interface conductance across an interface. To better understand this effect, extensive experimental measurements of h were made for a nonconforming interface of solid beryllium and stainless steel.

II. EXPERIMENTAL SETUP

The basic experimental apparatus in the BaS configuration is shown in Fig. 3, and consists of (from top to bottom) an electrically powered heater block to generate the requisite heat flux, a flux smoother to straighten the heat flow lines, the beryllium specimen, the Type 316 stainless steel specimen, an aluminum heat flux meter to measure the magnitude of the heat flux, and a cooling block to reject the heat. All components of the test article were located within a bell jar so that measurements could be made in vacuum or with gases other than air. There were three versions of the test apparatus corresponding to three diameters of test specimens (1, 2, and 3 in.). All three versions worked on the exact same principle, and only the dimensions of the various components were different. The relative direction of heat flow across the beryllium-Type 316 stainless steel interface was controlled by arranging the test specimens in the BaS configuration or in the SaB configuration.

II.A. Beryllium Specimens

The beryllium specimens were circular disks of S-200f-grade solid beryllium measuring 0.25-in. thick and possessing diameters of 1.00, 2.00, or 3.00 in. One surface of each beryllium disk was machine cut and coated with a silicone-based thermal grease to minimize the interface resistance between the beryllium specimen and the adjacent heat flux smoother. The test surface (that in contact with the steel specimen) of each disk was machine cut and then either lapped, sand blasted, or ballbearing blasted to a surface roughness of ~0.1, 1, and 10 μm, respectively.

One 0.0135-in. hole was radially drilled (using a number 80 carbide drill) into each of the beryllium specimens so that a single 0.010-in.-diam sheathed K-type thermocouple could be installed in each disk. The thermocouple hole was located 2.50 mm from the test surface. Beryllium thermal conductivity data were obtained from the Brush-Wellman Corporation.[4]

II.B. Type 316 Stainless Steel

The Type 316 stainless steel specimens were identical to the beryllium specimens with regard to thickness, diameter, and location of the thermocouple hole. The test surface (that in contact with the beryllium disk) of each disk was machine cut and lapped to a surface roughness of ~0.2 μm. Because of the limited accuracy of the data reported in the literature, the thermal conductivity of the Type 316 stainless steel was measured as a function of temperature in a separate experiment outlined in Abelson's PhD thesis.[3]

II.C. Heater Block, Electrical Heating Band, and Heat Flux Limiter

An electrical heating band produced the required heat flux through the beryllium and Type 316 stainless steel specimens. The heater had a maximum power output of 550 W and a maximum operating temperature of 482°C (900°F). To minimize conductive heat losses and thereby maximize the heat flow across the beryllium-Type 316 stainless steel interface, a "heat flux limiter" was positioned between the heater block and the top support structure (Fig. 3). Essentially a thermal insulator, this component was a cylindrical piece of low-thermal conductivity material with a reduced-diameter neck to increase its thermal resistance.

II.D. Aluminum Heat Flux Meter

The magnitude of the heat flux through the beryllium and steel specimens was determined by measuring the temperature difference along a precisely known length of aluminum rod and using Fourier's law of heat conduction. The thermal conductivity of aluminum was measured as a function of temperature in the author's PhD thesis.[3]

II.E. Heat Sink

The heat sink assembly was a 2-in.-diam by 1.8-in.-tall cylindrical copper "cup" wrapped with five turns of

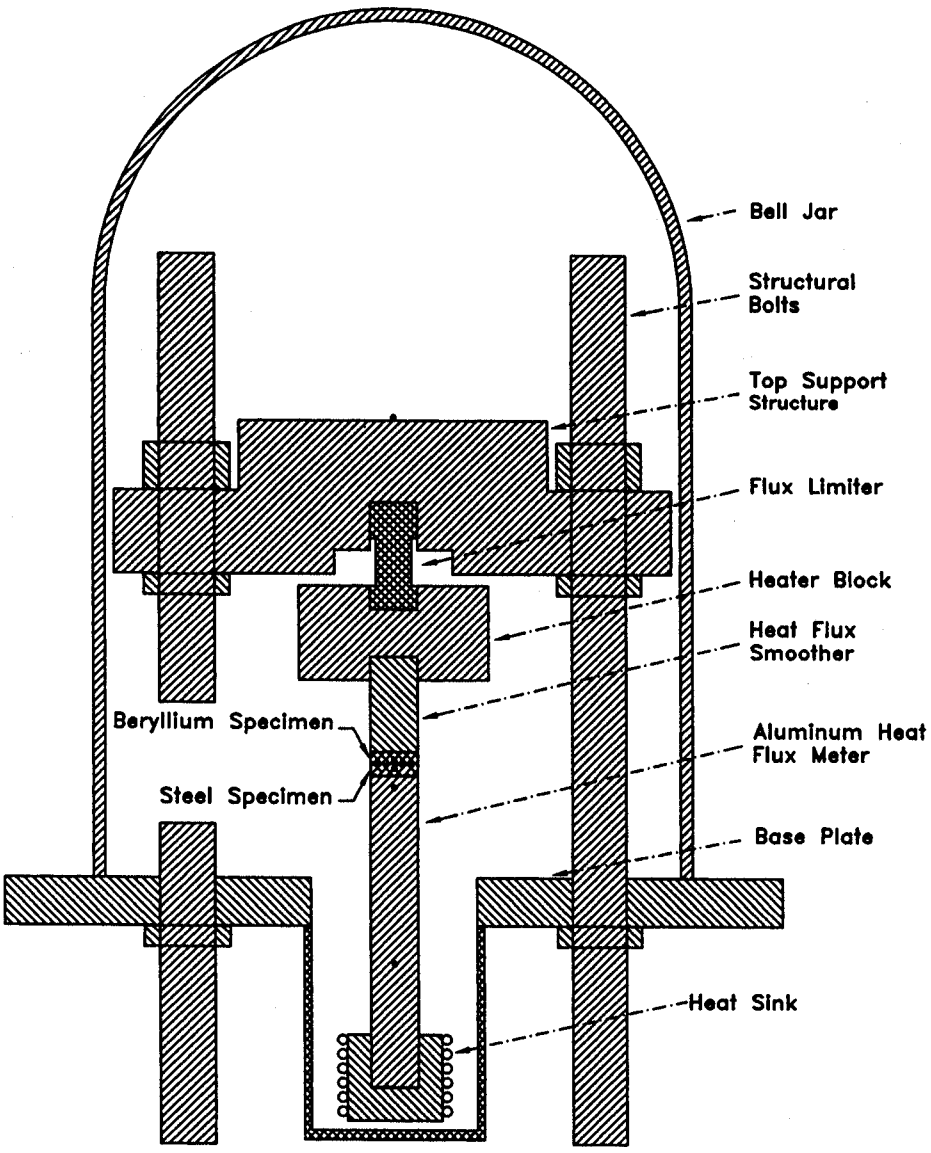

Fig. 3. Test article design for 1-in.-diam specimens.

0.25-in. inside diameter (i.d.) copper tubing. Water with an inlet temperature of ~15°C was used as the coolant.

II.F. Vacuum Chamber, Vacuum Pump, Hydraulic Press, and Load Cell

The vacuum chamber was a glass bell jar,[a] measuring 18-in. high by 12 in. in diameter, resting on top of an 16- × 16- × 1-in. aluminum baseplate (Fig. 3). A vacuum pump[b] was used to achieve gas pressure as low as 100 mTorr. A stainless steel bellows connected the underside of the baseplate to a hydraulic laboratory press.[c] All contact pressure measurements were made utilizing an electronic load cell[d] connected to a digital process indicator.

II.G. Pressure Gauges and Gas Pressure Regulation

Two different pressure transducers were used to measure the chamber gas pressure. For runs conducted in helium above a gas pressure of 10 Torr, an absolute pressure gauge[e] was used. For runs performed in helium below 10 Torr, or in air for any gas pressure, a Convectron gauge[f] was utilized.

[a] Pyrex brand.
[b] A Welch model 1400.
[c] From Carver, model C.
[d] Omega brand.
[e] MKS Baratron type 122A.
[f] Model 275.

An electronic proportioning control valve[g] was used to control the gas pressure within the vacuum chamber. The gas feed to the proportional valve came from a high-pressure gas cylinder fitted with a pressure regulator.[h] The regulator was set to 5 psig. When the proportional valve was in a feedback loop with the Baratron and Convectron pressure gauges, the gas pressure within the bell jar was typically accurate to within 5% of any value selected by the user.

II.H. Thermocouples and Thermocouple Vacuum Passthrough

All temperature measurements were made with 0.010-in., sheathed K-type thermocouples.[i] All thermocouples were calibrated in an ice bath prior to installation in the test apparatus. Numerous temperature measurements were made of the bath, and the mean and standard deviations of the readings computed. The difference between each average thermocouple measurement and the ice bath temperature was treated as a bias error and simply added or subtracted from every temperature measurement made from that particular thermocouple (effectively eliminating the bias error component). The standard deviation of the thermocouple measurements served as the random error for that particular thermocouple.

II.I. Data Acquisition System

All temperature and pressure measurements were read into a PC and processed by a digital acquisition board[j] (DAQ) and LabView software. The DAQ board possessed a 16-bit digital-to-analog converter that accepted up to six pairs of K-type thermocouple leads and two pairs of voltage leads coming from the pressure transducers. The DAQ system was also utilized to monitor and control the gas pressure within the bell jar. An analog output board,[k] with 12-bit resolution, was used to generate the analog output voltage required to control the proportional-flow control valve.

II.J. Thermal Insulation

All three interface conductance test articles (1-, 2-, and 3-in. diameters) were insulated with a 2-in.-thick layer of high-temperature fiberglass insulation, surrounded by aluminum foil, to minimize both convective and radiative heat losses. The insulation possessed a thermal conductivity of 0.033 W/m·K at room temperature and could operate in environments ranging from 0 to 850°C.

[g]Omega PV series.
[h]Liquid brand.
[i]Acquired from Omega Industries.
[j]National Instruments model AT-MIO-16XE-10.
[k]National Instruments model AT-AO-6.

II.K. Surface Profilometry

Microscopic surface profilometry was performed on all 14 beryllium and stainless steel test surfaces after all measurements were made. Three 1-cm-long traces, consisting of 2000 height measurements per trace, were obtained for each surface using a profilometer[l] attached to a PC. The resultant data were processed using a commercial spreadsheet program to extract the root-mean-square (rms) roughness of each surface. The asperity-height distribution was checked for randomness by comparing it with a Gaussian height distribution possessing the same mean and standard deviation as each test surface. Asperity-height histograms for the three 1-in.-diam beryllium disks are presented in Figs. 4a, 4b, and 4c with associated normal distributions. Table I lists the rms surface roughness for each of the 14 test surfaces.

III. THEORY OF OPERATION

There are four steps to calculating h using the interface conductance test apparatus. The first step is to determine the heat flux q flowing across the test interface. This is accomplished via Fourier's law:

$$q = k_{\mathrm{Al}} \frac{T_3 - T_4}{L_{3-4}} \quad . \tag{2}$$

In this equation, T_3 and T_4 are two temperatures measured along the length of a cylindrical aluminum rod (Fig. 1). The value L_{3-4} is the length between these two thermocouples, and k_{Al} is the thermal conductivity of the aluminum.

Next, the interfacial-surface temperature of the beryllium specimen, T_i^{Be} is computed. The value T_i^{Be} is not a directly measurable quantity, so its value must be extrapolated from another location (thermocouple 1 in Fig. 1) using the relation

$$T_i^{\mathrm{Be}} = T_1 - \frac{q \cdot L_{1-i}}{k_{\mathrm{Be}}} \quad , \tag{3}$$

where

T_1 = thermocouple-measured temperature at a known point within the beryllium specimen

L_{1-i} = distance between the aforementioned thermocouple and the test interface

k_{Al} = thermal conductivity of the beryllium specimen.

The interfacial-surface temperature of the steel specimen T_i^{Steel} is computed via Eq. (4), where T_2 is the thermocouple-measured temperature at a known point within the steel specimen, L_{i-2} is the distance between

[l]Tencor brand.

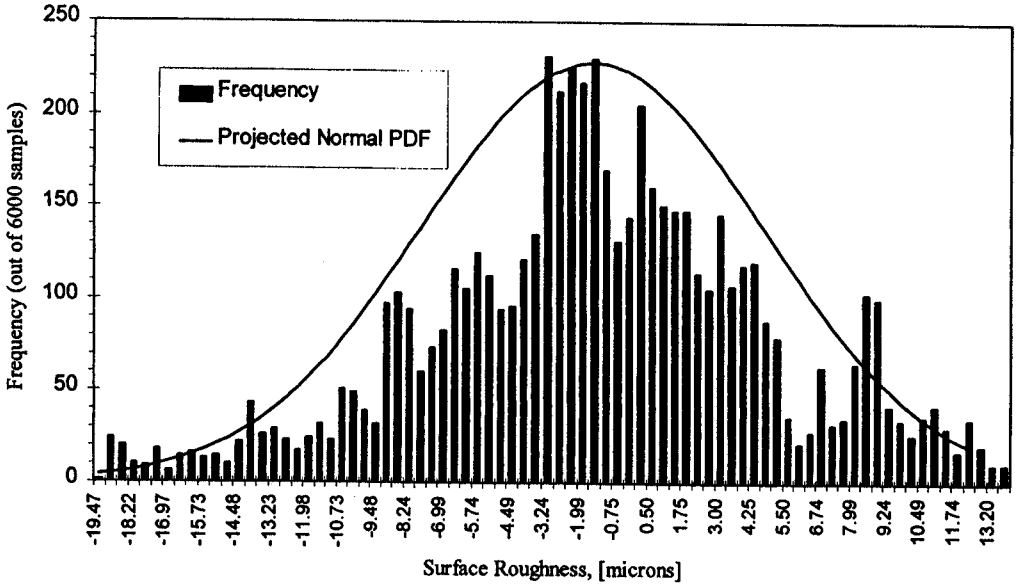

Fig. 4a. Asperity height histogram and projected normal distribution for the 1-in.-diam ball-bearing-blasted beryllium disk (1σ = 6.25 μm).

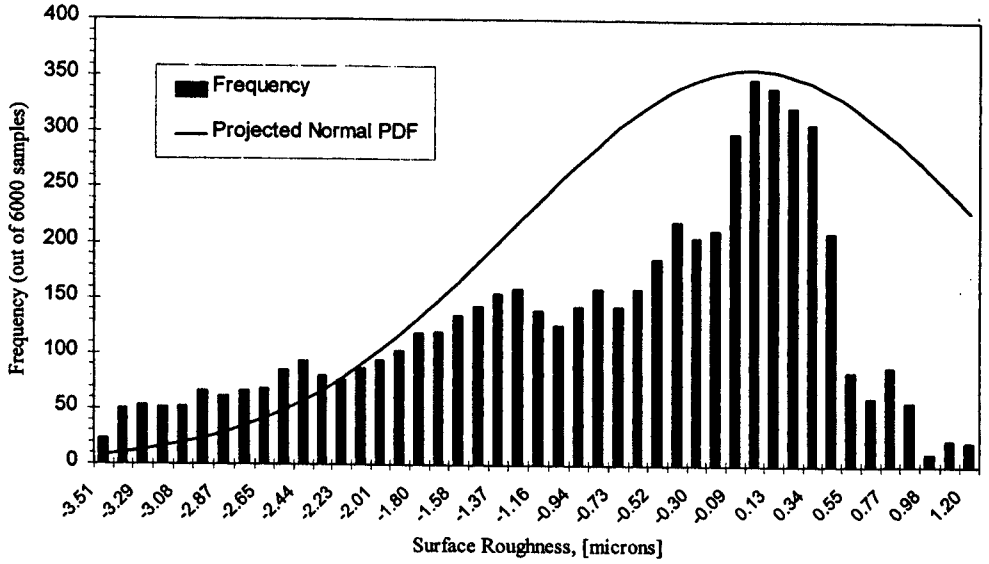

Fig. 4b. Asperity height histogram and projected normal distribution for the 1-in.-diam sand-blasted beryllium disk (1σ = 1.28 μm).

the test interface and the aforementioned thermocouple, and k_{Steel} is the thermal conductivity of the steel specimen:

$$T_i^{Steel} = T_2 + \frac{q \cdot L_{i-2}}{k_{Steel}} \quad . \tag{4}$$

Finally, having solved for q, T_i^{Be}, and T_i^{Steel}, the interface conductance can be determined from its defining relation:

$$h \equiv \frac{q}{T_i^{Be} - T_i^{Steel}} \quad . \tag{5}$$

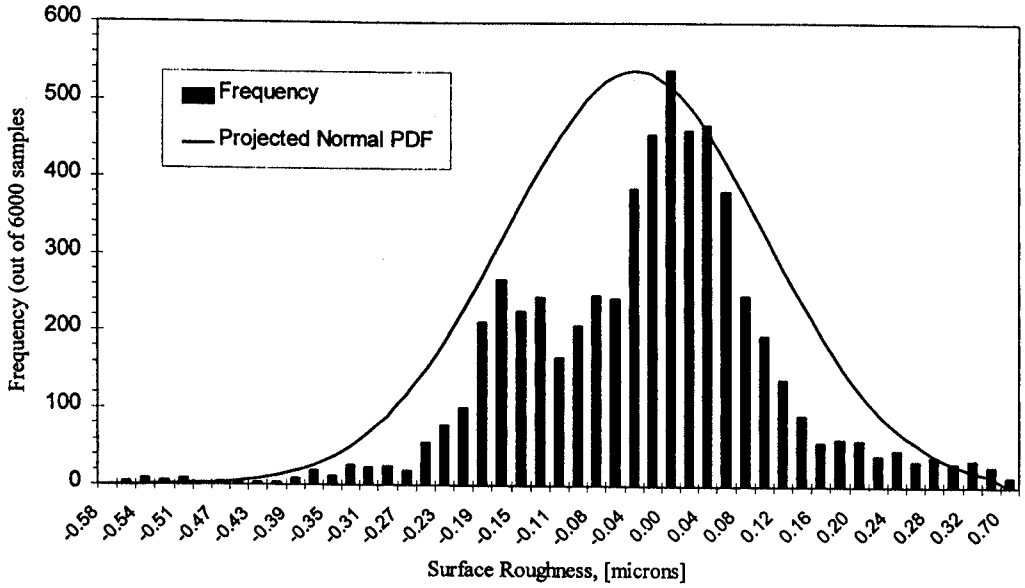

Fig. 4c. Asperity height histogram and projected normal distribution for the 1-in.-diam lapped beryllium disk ($1\sigma = 0.14\ \mu m$).

IV. INTERFACE CONDUCTANCE VERSUS CONTACT PRESSURE EXPERIMENTAL RESULTS

IV.A. Foreword

Interface conductance was measured as a function of contact pressure for 96 permutations of surface roughness, gas pressure, gas type, disk diameter, and disk configuration. In each case, the beryllium disk (whose roughness was varied) was mated against a polished steel disk of fixed surface roughness ($\sigma \approx 0.2\ \mu m$).

IV.B. Experimental Procedures

The procedure for collecting the interface conductance data was to first evacuate the bell jar to a pressure of ~200 mTorr and unload the hydraulic press. The electric heater was then turned on and the system allowed to reach steady state (this step typically took 3 h or more to accomplish). Once a steady value of h was achieved, its value was recorded. Next, the contact pressure was increased by a fixed amount and the system allowed to reach the new steady value of interface conductance. This procedure was continued until the maximum contact pressure of 11.62 MPa was reached, whereupon the test article was unloaded and the bell jar filled with 76 Torr of helium gas. The contact pressure was increased again in increments, always allowing h to reach a steady value before recording its magnitude. The helium pressure was increased to 760 Torr, and the cycle repeated. On completion of the two helium runs, the bell jar was evacuated again and backfilled with air, first at 76 Torr and then at 760 Torr, analogous to the helium runs.

TABLE I

Mean Asperity Heights for the Beryllium and Type 316 Stainless Steel Test Surfaces

Specimen Name	Roughness (μm)	Specimen Name	Roughness (μm)
1-in.-diam, ball-bearing-blasted beryllium disk	6.25	1-in.-diam, lapped Type 316 stainless steel disk 1	0.21
1-in.-diam, sand-blasted beryllium disk	1.28	1-in.-diam, lapped Type 316 stainless steel disk 2	0.38
1-in.-diam, lapped beryllium disk	0.14	1-in.-diam, lapped Type 316 stainless steel disk 3	0.24
2-in.-diam, ball-bearing-blasted beryllium disk	10.7	2-in.-diam, lapped Type 316 stainless steel disk 1	0.32
2-in.-diam, sand-blasted beryllium disk	0.10	2-in.-diam, lapped Type 316 stainless steel disk 3	0.17
3-in.-diam, ball-bearing-blasted beryllium disk	10.1	3-in.-diam, lapped Type 316 stainless steel disk 1	0.29
3-in.-diam, sand-blasted beryllium disk	0.075	3-in.-diam, lapped Type 316 stainless steel disk 3	0.36

Once all of the data was taken (in vacuum, helium, and air), the test article was disassembled and the disk surfaces inspected for oxidation or outgassing products. A slight amount of oxidation was observed on the Type 316 stainless steel surfaces after the air runs and was easily removed with a commercially available metal polish. Often, a second set of runs was taken to check for repeatability of the first set of h measurements. Generally, the two sets of data showed excellent agreement.

For runs carried out under gas pressures of 200 mTorr, the type of gas used (i.e., air or helium) had no impact upon the magnitude of the interface conductance. Furthermore, based on the experimental results, the contribution of the gas layer to interfacial heat transport was negligible at such low values of gas pressure. Therefore, to simplify the text, we will not distinguish between runs conducted in 200 mTorr of air and in 200 mTorr of helium. Rather, they will both be referred to as being conducted in vacuum.

IV.C. Verification Experiment

Interface conductance measurements made with the current test apparatus were compared with similar measurements made in Abelson's earlier work,[5] Fig. 5. This was done to determine whether the new test rig could accurately repeat the previous h measurements and, by doing so, generate confidence that no gross design errors or construction flaws existed for said test apparatus. The test specimens used in Ref. 5 were lapped-beryllium and Type 304 stainless steel disks, arranged in the BaS configuration, with a combined surface roughness of 0.56 μm. The specimens used in the current work were lapped-beryllium and Type 316 stainless steel disks (also in the BaS configuration) of 0.28-μm surface roughness. The details of the test rig used in Ref. 5 are described in Abelson's MS thesis[6]; the previous rig was constructed entirely by graduate students other than this author.

Figure 5 demonstrates that there is very good agreement between the interface conductance results obtained from both Abelson's previous test rig and the test rig specified in this paper. Measurements were made in 760 Torr of helium and in lower gas pressures (76 Torr He for the present data set and 98 Torr He for the data taken from the author's earlier work). The present results were marginally higher than those from Ref. 5, which was expected since the present test specimens have a somewhat lower surface roughness (0.28 versus 0.56 μm). Additionally, the uncertainty in the experimental results ranged from 10 to 20% [using the treat everything random (TER) methodology] or from 20 to 40% [using the distinct bias and random error (DBRE) methodology]. The magnitude of these errors was more than enough to account for the difference between the two sets of interface conductance data.

In summary, the experimental results were very similar even though tests were conducted using two different sets of specimens in two different test rigs built by different people. This suggests that the results were repeatable, that there were no gross errors in design or construction in the current test rig, and that there is confidence

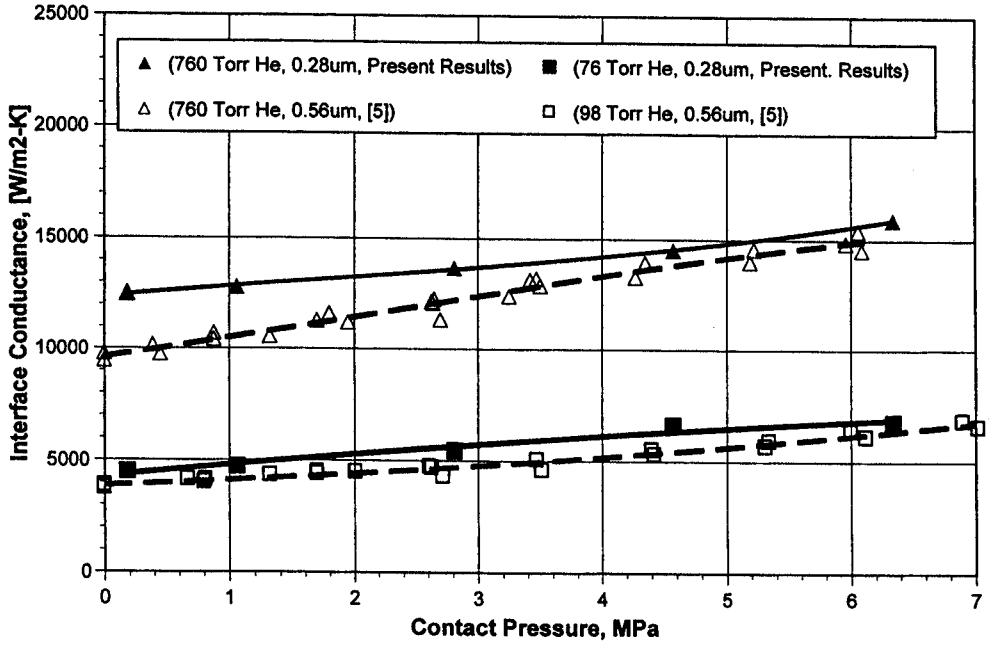

Fig. 5. Verification experiment results for current test article, h versus P_c, helium gas, lapped beryllium and stainless steel.

that any interface conductance measurements made with said test rig should be as accurate as specified in the error analysis section of this work, Sec. VI.

IV.D. Experimental *h* Versus *Pc* Data

Four sets of experimental measurements were made with the steel-beryllium disks. The first set were for 1-in.-diam disks in the SaB configuration where the heat flux travels from the steel disk to the beryllium disk. Because of the effects of nonconforming thermal expansion, the interfacial contact area for disks in the SaB configuration is expected to be an annular region located about the outer perimeter of the disks (Fig. 2a). Three beryllium disks of varying degrees of surface roughness were used and runs were carried out in helium and air. The combined surface roughnesses of each of the three beryllium-Type 316 stainless steel disk pairs was 6.25, 1.34, and 0.28 μm.

The second set of measurements were for the same three 1-in.-diam disks as mentioned earlier, but in the BaS configuration. The typical interfacial contact area for this configuration is expected to be a concentrically located circle, (Fig. 2b). The third set of runs are for two pairs of 2-in.-diam disks, with combined surface roughnesses of 10.7 and 0.20 μm in the SaB configuration.

The last set of measurements were for two pairs of 3-in. diam disks in the SaB configuration, with combined surface roughnesses of 8.78 and 0.28 μm in the SaB configuration. An exhaustive pre-experimental error analysis was presented in one author's PhD thesis[3] and governed the design of the test article. A post-experimental error analysis is presented later in this paper.

IV.E. Discussion of the *h* Versus *Pc* Results

The interface conductance was observed to be a strong function of contact pressure, as expected. This is because the application of a compressive axial force on the beryllium-steel specimens forces the two surfaces closer to each other via deformation of the surface asperities and in macroscopic deflection of the disk profiles. For interfaces formed from very rough surfaces (>6 μm), the magnitude of h appears to be less sensitive to increases in contact pressure than for interfaces formed from smoother surfaces (<2 μm). This suggests that rougher surfaces can create more robust interfaces which, at the expense of having lower overall magnitudes of h, possess more uniform values of interface conductance over wider ranges of contact pressure.

Typically, the interface conductance experienced a significantly larger increase in value when the gas pressure was raised from 76 to 760 Torr as opposed to when it was raised from vacuum (200 mTorr) to 76 Torr (Fig. 6). In helium gas, for example, the magnitude of h (for the

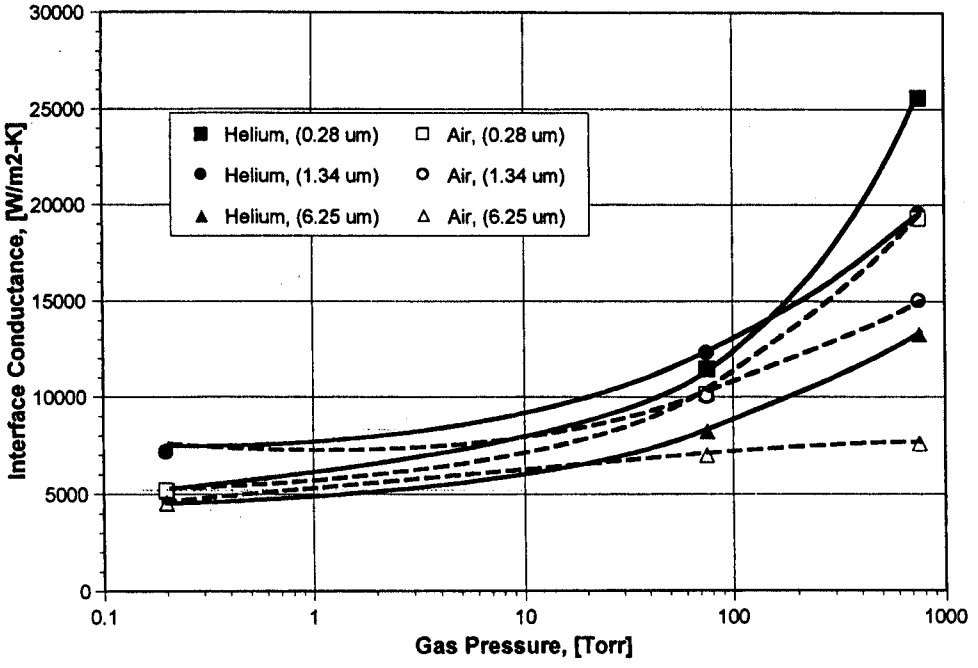

Fig. 6. Interface conductance versus gas pressure, helium and air, various surface roughnesses, P_c = 6.16 MPa, 1-in. disks, SaB orientation.

0.28-μm surface) was raised by 6300 and 14 140 W/m^2·K as the gas pressure was increased from 0.2 to 76 Torr and from 76 to 760 Torr, respectively. Thus, not only did the absolute value of h increase with gas pressure, but so did the sensitivity of h to P_g. The magnitude of this sensitivity was a function of the surface roughness of the test specimens as indicated by the 6.25-μm specimens, which (in helium) experienced only a 3700 and a 5050 W/m^2·K increase in value as the gas pressure was raised over the same intervals as the 0.28-μm specimen mentioned earlier. Thus, rougher surfaces have values of interface conductance that are less sensitive to variations in gas pressure.

Runs conducted in air generally yielded lower overall values of interface conductance than runs performed in helium (Fig. 6). Furthermore, the sensitivity of h to gas pressure was smaller in air than in helium. Take, for instance, the 0.28-μm specimen: Increasing the air pressure from 0.2 to 76 Torr raised h by 4950 W/m^2·K (compared with 6300 W/m^2·K in helium). When the air pressure was increased from 76 to 760 Torr, the value of h was raised by 9150 W/m^2·K, which is only 65% of the increase in h observed in helium gas under analogous conditions. For the 6.25-μm surface, the sensitivity of h to the air pressure all but vanished for P_g greater than 76 Torr.

Interface conductance was observed to be relatively insensitive to disk diameter for rough beryllium surfaces (>6 μm) (Fig. 7), consistent with the results reported by Berman.[7] This implies that the observed results should hold true for disk diameters exceeding 3 in., as long as the beryllium surface roughness is of the order of 6 μm or greater. One reason for this result may be that very rough surfaces have asperity heights that are greater than the macroscopic gap spacing incurred by nonuniform thermal expansion. These asperities would act as a compliant layer, filling the macroscopic gaps that would typically reduce the interface heat conductance of smoother surfaces.

For interfaces formed from very smooth beryllium surfaces (<0.4 μm), the magnitude of the interface conductance was a function of specimen diameter for a given value of gas pressure (Fig. 8). As the disk diameter was raised from 1 to 2 in., there was a noticeable raise in h. However, as the diameter was further increased from 2 to 3 in., the raise in h was only minimal, implying that a saturation effect was in process. Very smooth surfaces (i.e., lapped or polished) were expected to have asperity heights that were substantially smaller (an order of 0.1 μm) than the height of the macroscopic gap (an order of 1 to 10 μm). Because these small surface asperities could not act as a compliant layer and fill the gap, the interface conductance became sensitive to the geometry of the interfacing surfaces. The data suggest that as the disk diameter was increased, the test surfaces were flattened against one another, decreasing the mean separation distance and increasing the magnitude of h. This seems reasonable since larger-diameter disks are less rigid than smaller-diameter disks for a given thickness. This would explain the relatively low values of h observed for the 1-in. specimens relative to the 2- and 3-in.-diam specimens.

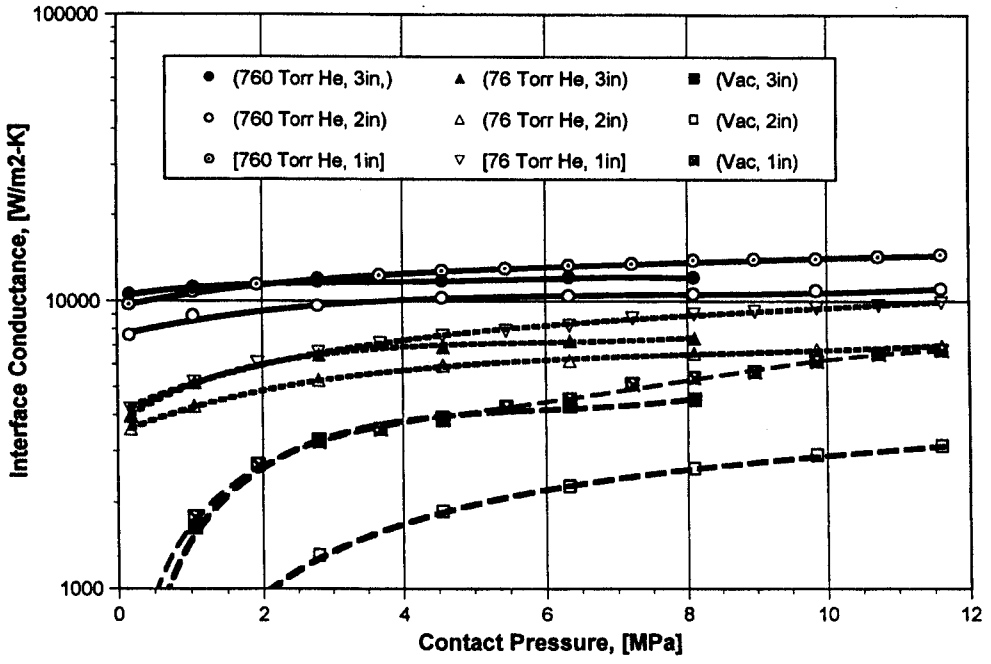

Fig. 7. Interface conductance versus contact pressure, all diameters, combined surface roughness >6 μm, helium gas, SaB configuration.

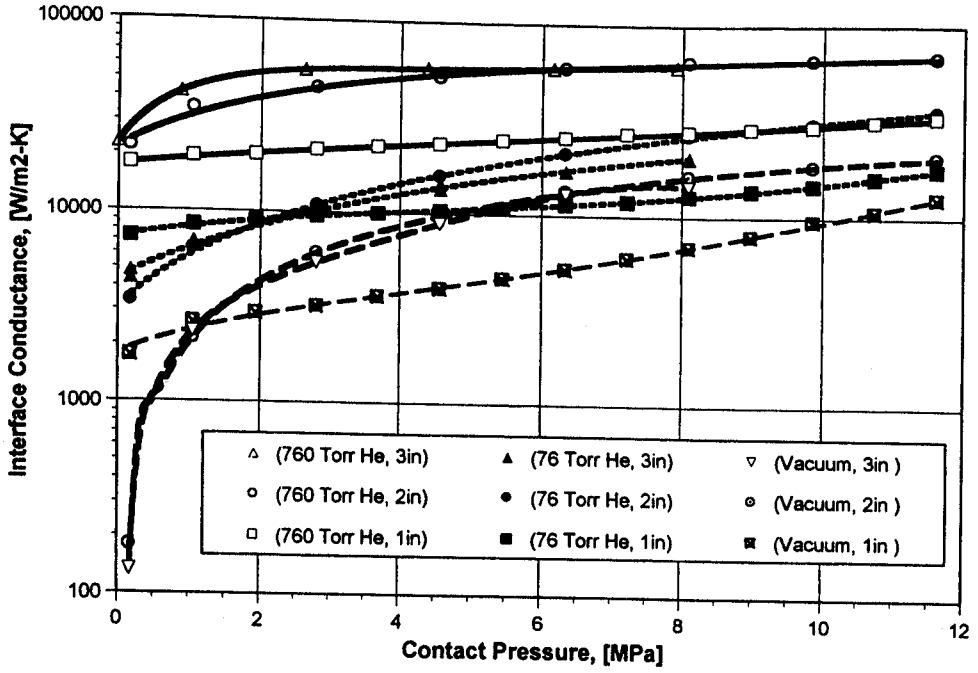

Fig. 8. Interface conductance versus contact pressure, all diameters, combined surface roughness <0.4 μm, helium gas, SaB configuration.

When the gas conductance component h_g of the interface conductance h was calculated, from $h = h_g + h_c$, where h_c is just h measured in vacuum, several significant trends were observed for the ball-bearing-blasted surfaces (>6 μm). First, h_g was nearly independent of contact pressure (Fig. 9). This implies that increasing P_c typically only affects the contact conductance h_c presumably by increasing the amount of surface-to-surface contact

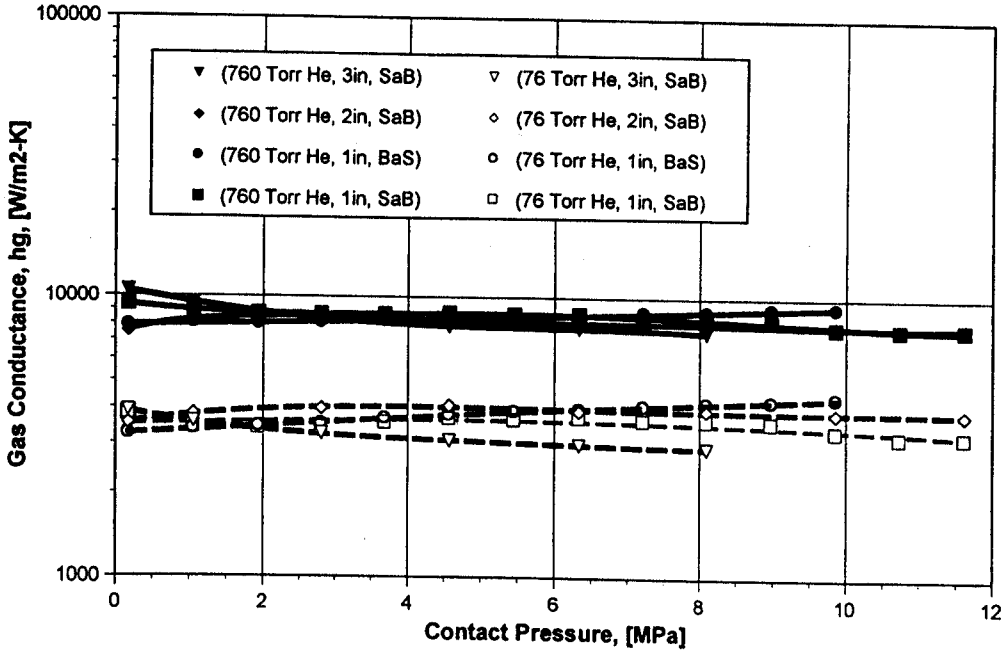

Fig. 9. Gas conductance versus contact pressure, helium gas, all disk diameters and orientations, roughness >6 μm.

area between the beryllium and steel surfaces. Second, raising the gas pressure from 76 to 760 Torr increased the magnitude of h_g by a relatively fixed amount of 5000 W/m^2·K. The size of this increase was insensitive of disk diameter and direction of heat flux (i.e., SaB and BaS configurations). Third, the gas conductance was only weakly sensitive to the magnitude of the disk diameter. The uncertainty in the data, however, is great enough that h_g may be completely independent of disk diameter. Higher accuracy interface conductance measurements are needed to confirm this.

Examining the gas conductance component of h for very smooth surfaces (<0.4 μm), the value of h_g was typically insensitive to the magnitude of the contact pressure (Fig. 10). Increasing the disk diameter from 1 to 2 in., in 760 Torr of helium, raised the mean value of the gas conductance by ~170%. Further increasing the disk diameter from 2 to 3 in. appeared to have little impact on h_g, suggesting that the magnitude of the gas conductance saturated above a certain value of disk diameter. Raising the gas pressure from 76 to 760 Torr increased the mean value of h_g by ~25 000 W/m^2·K. Comparing this increase with the 5000 W/m^2·K increase observed for the roughened beryllium surface (>6 μm), it was clear that the gas conductance was very sensitive to surface roughness.

Interface conductance was found to be dependent on disk orientation (SaB or BaS) and, thus, on the direction of heat flow, with SaB corresponding to heat flow from the steel disk to the beryllium disk and vice versa. The direction of heat flow determined which portion of the two test surfaces would be in contact due to nonuniform thermal expansion. For example, it was expected that the test specimens would experience annular surface contact along their outer perimeter in the SaB configuration; whereas, in the BaS configuration, the specimens experienced concentric contact. Since the disk-deflection profile was different for each of these two cases, one might expect that the contact conductance h_c would be dependent on the direction of the heat flux. This is, in fact, what was observed (Fig. 11). The discovery of a directional effect is not new; in fact, it was first noted by Starr[8] in 1936 and subsequently by numerous other investigators.[9–13] While many of the reported occurrences were for interfaces formed from dissimilar materials, Thomas and Probert[14] performed experiments with similar materials (steel-steel) and still observed a directional effect, with the magnitude of h being as much as 70% greater for heat flow in one direction than in the opposite direction.

As Fig. 11 demonstrates, the contact conductance for the beryllium-steel interface in the SaB configuration can be >6600 W/m^2·K higher than for runs carried out in the BaS configuration. The implication is there is significantly more interfacial contact area for disks in annular contact rather than in concentric contact.

In conclusion, the magnitude of the interface heat conductance was found to be a strong function of surface roughness, gas pressure, and contact pressure. Increasing the gas pressure or contact pressure typically increased the magnitude of h, whereas raising the surface roughness generally reduced the value of h.

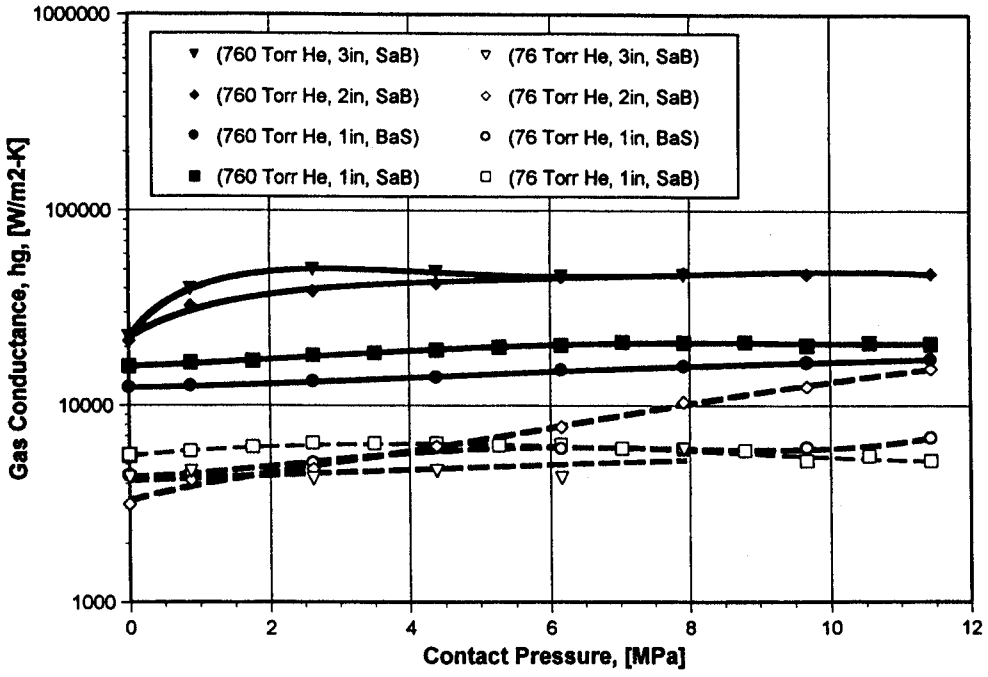

Fig. 10. Gas conductance versus contact pressure, helium gas, all disk diameters and orientations, roughness <0.4 μm.

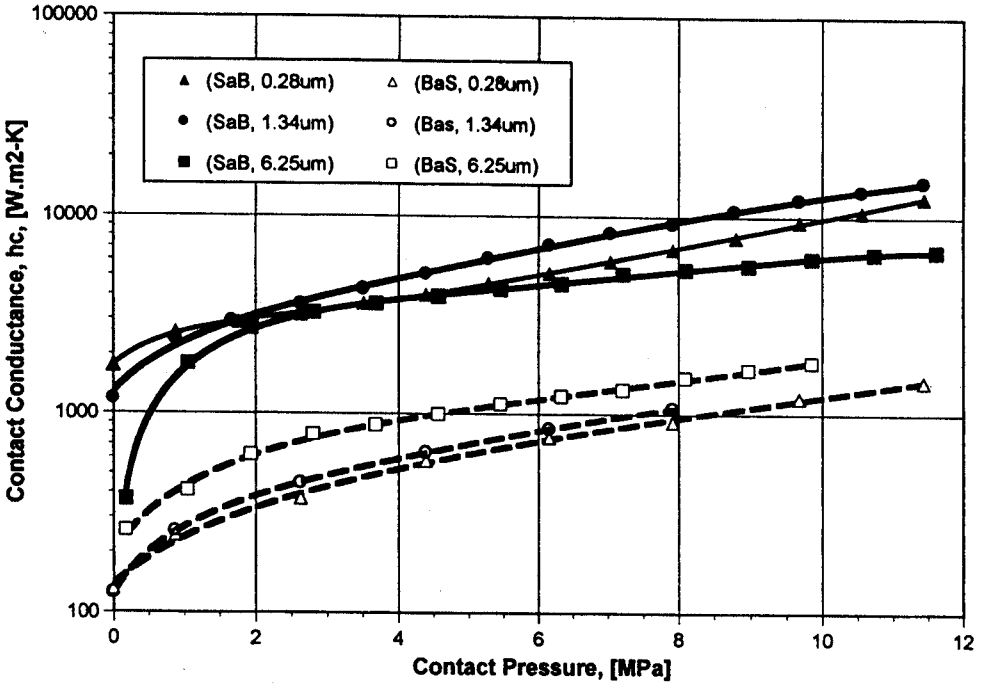

Fig. 11. Contact conductance versus contact pressure, 1-in. disks, various surface roughnesses, both disk orientations.

Measurements carried out in helium tended to yield larger values of h than runs carried out in air, due to helium's greater thermal conductivity, with the difference increasing as the gas pressure was raised. For very rough surfaces, h was nearly independent of disk diameter and contact pressure. However, very smooth surfaces showed that h increased as the disk diameter was increased. A directional effect was observed in the magnitude h with respect to heat flux. Disks arranged in the SaB configuration typically yielded larger values of interface conductance than disks in the BaS configuration.

V. EXPERIMENTAL RESULTS FOR INTERFACE CONDUCTANCE VERSUS HEAT FLUX

V.A. Foreword

Interface conductance was measured as a function of heat flux for numerous values of surface roughness, helium gas pressure, contact pressure, and disk orientation. Measurements were made with the beryllium and steel disks in both the SaB and BaS configurations to determine what effect the heat flux direction would play on the magnitude of h. All runs were performed using the 1-in.-diam specimens.

V.B. Experimental Procedures

The general test-taking procedure was to first evacuate the test chamber to a gas pressure of <200 mTorr and then turn on the electric heater and adjust it to a heat flux of ~10 to 20 kW/m^2. The temperature profile of the test article was then allowed sufficient time to reach steady state (often requiring 2 to 3 h to do so) before any data were recorded. Once steady state was achieved, as determined by real-time plots of heat flux and interface conductance via a digital acquisition system, the magnitudes of h and q were recorded. The contact pressure was then increased to 5 MPa and held there until the test article reached a new steady-state temperature profile (this generally took 45 min to 1 h to complete), whereupon the relevant data were recorded. The contact pressure was then increased to 10 MPa, and the steady values of h and q recorded. The test rig was unloaded (back to 0.18 MPa), and the heat flux increased by a fixed amount, and the previous cycle repeated. The maximum heat flux used in the interface conductance measurements was governed by an upper limit of ~200 kW/m^2. However, with respect to runs performed in vacuum under 0.18 MPa of contact pressure, the maximum usable value of q was generally <200 kW/m^2 due to limits imposed by the maximum operating temperature of the heater element.

Once a complete set of data had been collected, the test article was disassembled and the test surfaces inspected for contamination (i.e., due to outgassing, oxidation, etc.). Since all runs were carried out either in vacuum or helium, there was no significant oxidation observed on the test surfaces. After inspection of the test surfaces was completed, the thermocouples were rechecked for calibration and then reinserted into the test

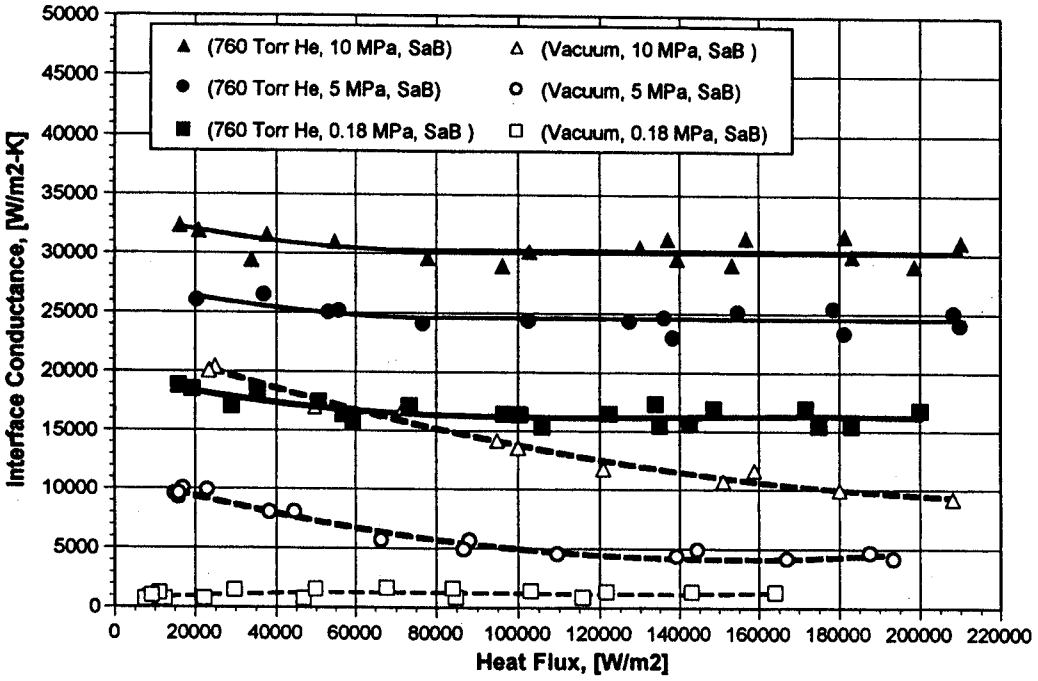

Fig. 12. Interface conductance versus heat flux, 760-Torr helium and vacuum, combined surface roughness = 0.28 μm, SaB configuration.

specimens. The previous interface conductance measurements were then repeated to ascertain whether thermocouple reinstallation or test rig reassembly altered the value of h. Typically, the two data sets agreed very closely.

V.C. Experimental h versus q Results

Interface conductance measurements for test surfaces in the SaB orientation are presented in Figs. 12, 13,

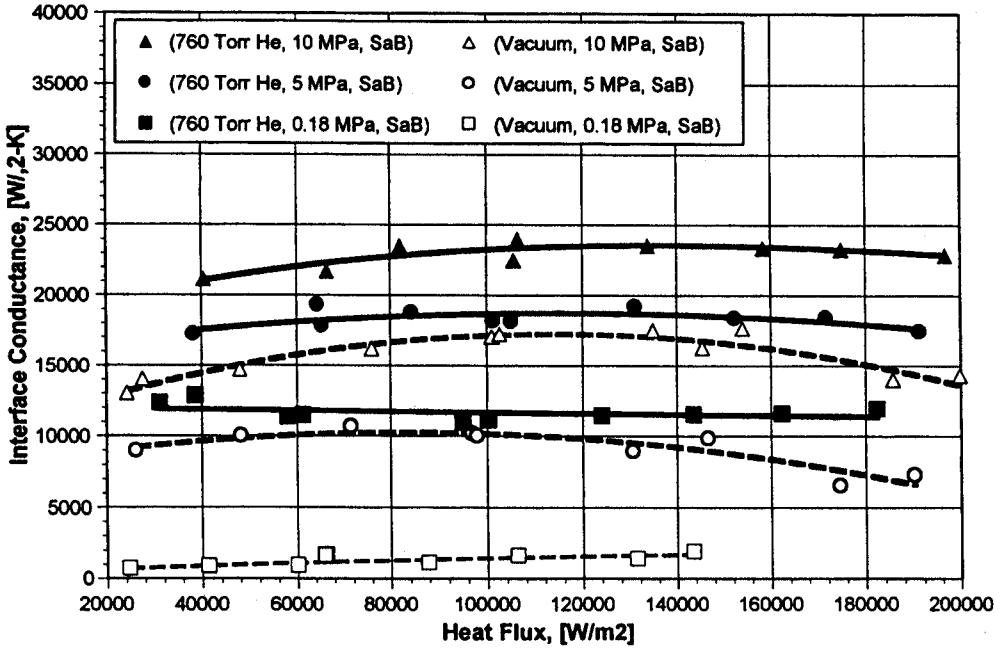

Fig. 13. Interface conductance versus heat flux, 760-Torr helium and vacuum, combined surface roughness = 1.34 μm, SaB configuration.

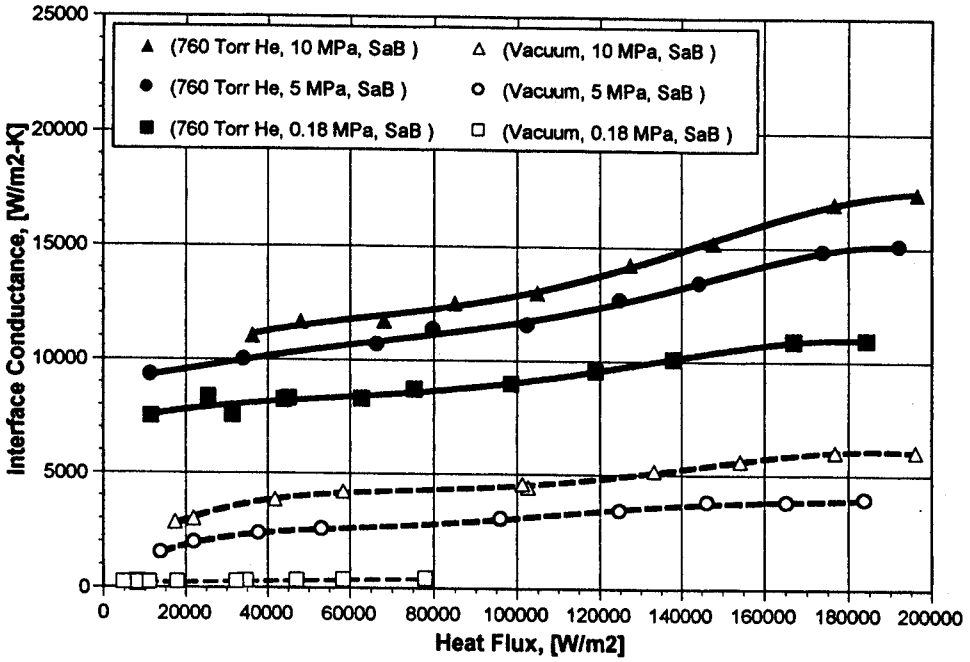

Fig. 14. Interface conductance versus heat flux, 760-Torr helium and vacuum, combined surface roughness = 6.25 μm, SaB configuration.

and 14 as a function of heat flux, helium gas pressure, contact pressure, and surface roughness. Figures 15, 16, and 17 present h measurements obtained from specimens in the BaS configuration.

When interface conductance measurements were made in 760 Torr of helium, results for the 0.28- and 1.34-μm specimens typically indicated only a weak dependence of h on the magnitude of q (Figs. 18 and 19).

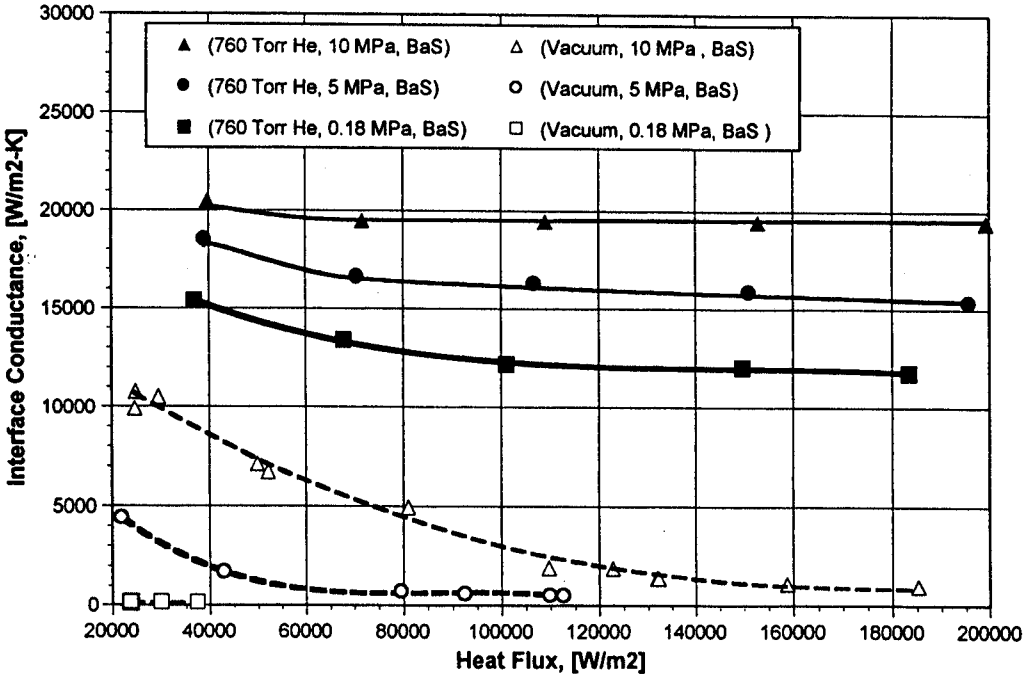

Fig. 15. Interface conductance versus heat flux, 760-Torr helium and vacuum, combined surface roughness = 0.28 μm, BaS configuration.

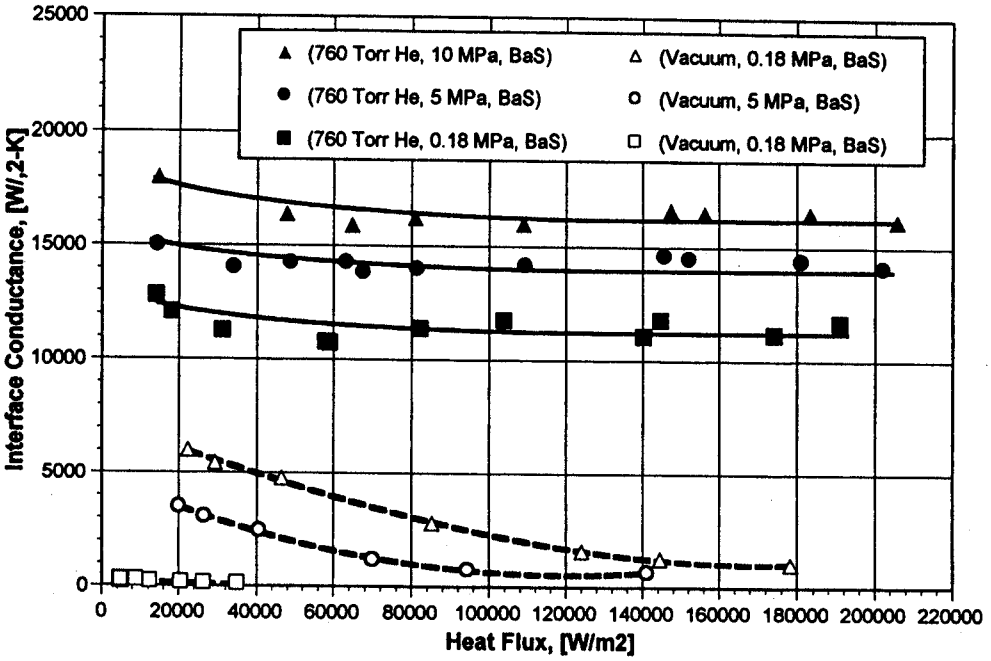

Fig. 16. Interface conductance versus heat flux, 760-Torr helium and vacuum, combined surface roughness = 1.34 μm, BaS configuration.

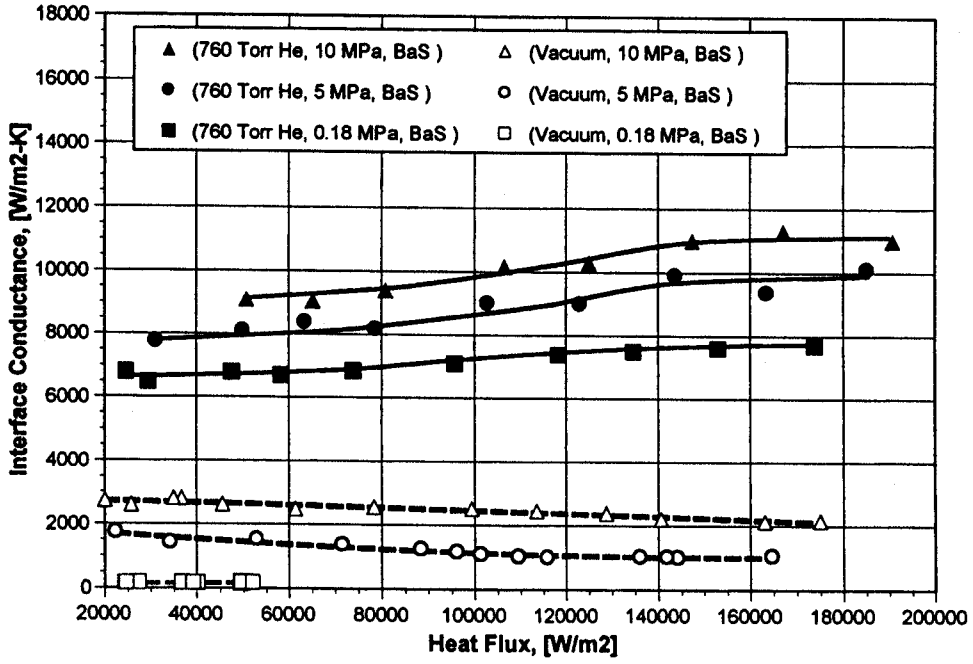

Fig. 17. Interface conductance versus heat flux, 760-Torr helium and vacuum, combined surface roughness = 6.25 μm, BaS configuration.

Specifically, the magnitude of the interface conductance was essentially independent of heat flux for values of q exceeding 50 kW/m^2. This result was found to be true regardless of the magnitude of the contact pressure or the direction of heat flow. For runs carried out with the rougher 6.25-μm test specimen (in 760-Torr He), the interface conductance showed a marginal tendency to increase in value as the heat flux was raised. However, the

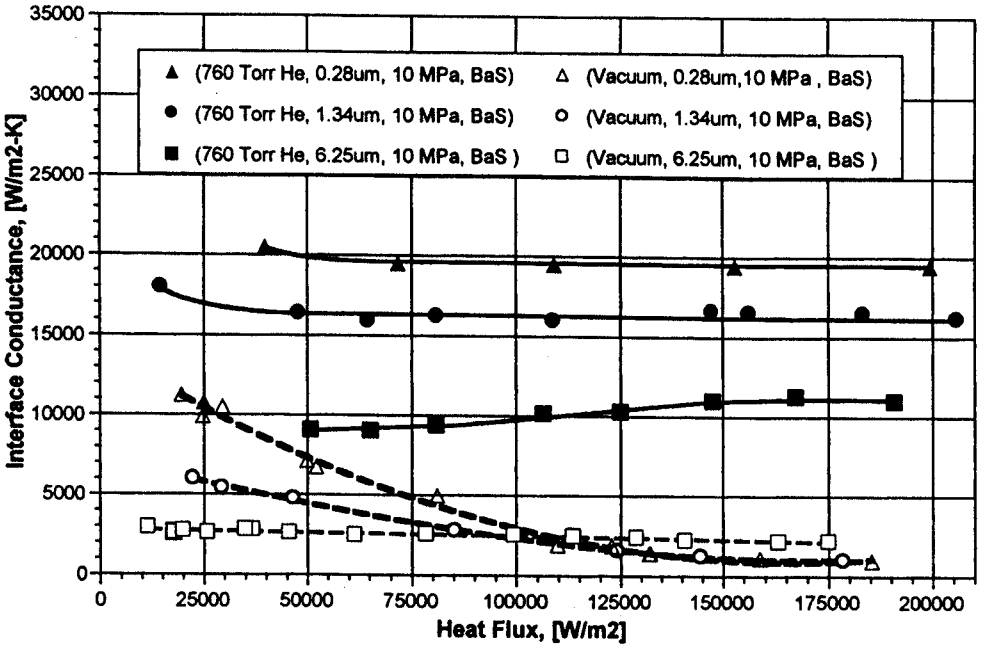

Fig. 18. Interface conductance versus heat flux, vacuum and 760-Torr helium, $P_c = 10$ MPa, all roughnesses, BaS configuration.

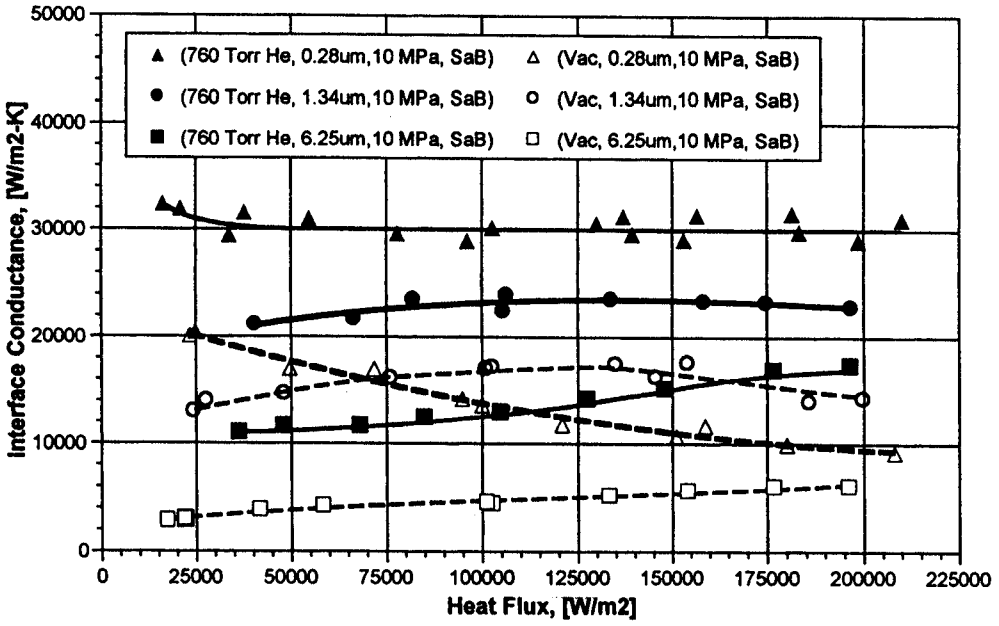

Fig. 19. Interface conductance versus heat flux, vacuum and 760-Torr helium, $P_c = 10$ MPa, all roughnesses, SaB configuration.

data suggest that the magnitude of h may saturate for heat fluxes exceeding 175 kW/m^2.

For runs conducted in vacuum, the interface conductance was generally found to be more sensitive to heat flux than when the same runs were performed in 760 Torr of helium (Figs. 18 and 19). Although this observation was found to be true for disks in both the SaB and BaS configurations, the latter configuration showed a higher degree of sensitivity (of h to q) than did the former. From these results, it is surmised that the presence of the interfacial gas layer acted to moderate the value of h, keeping it roughly uniform over the explored range of heat fluxes.

The magnitude of h for disks in the SaB configuration was generally higher than for disks in the BaS

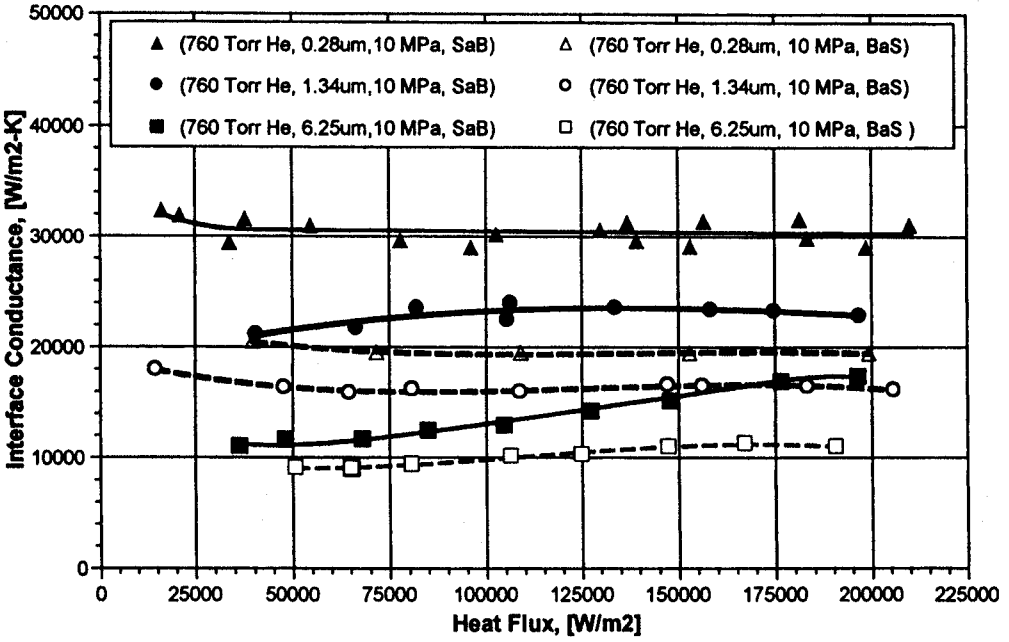

Fig. 20. Interface conductance versus heat flux, 760-Torr helium, P_c = 10 MPa, all roughnesses, SaB and BaS configurations.

configuration (Fig. 20). This is consistent with the findings from the previous h versus P_c data sets, and it may indicate that the area of interfacial contact is smaller in the BaS configuration than in the SaB configuration.

When the gas conductance h_g was computed for runs carried out with the 0.28- and 6.25-μm disks, it was discovered that the magnitude of h_g is only a weak function of disk configuration (SaB or BaS), but is a strong

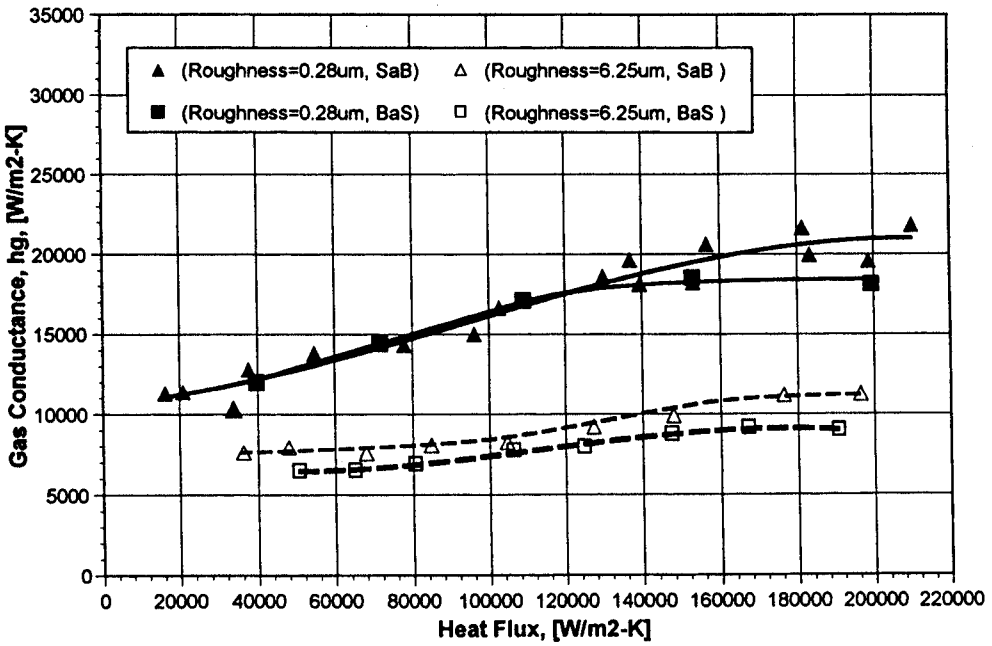

Fig. 21. Gas conductance versus heat flux, 760-Torr helium, P_c = 10 MPa, 1-in. disks, surface roughness = 0.28 and 6.25 μm, SaB and BaS orientations.

function of surface roughness (Fig. 21). Additionally, the value of the gas conductance increases with heat flux, although there is evidence that it reaches a steady value once q is raised beyond 180 kW/m^2.

When measurements were carried out in 760 Torr of helium, the ratio between h measured under 5 MPa and under 0.18 MPa of contact pressure was found to equal ~1.5, independent of surface roughness and disk orientation (Fig. 22). Similarly, the ratio of h under contact pressures of 10 and 5 MPa was discovered to be fixed at ~1.2. From these results, it is surmised that the presence of the interstitial gas layer desensitizes the relative increase in h (due to a fixed rise in contact pressure) to the surface characteristics of the test disks (surface roughness and disk orientation). The rate of increase in the ratio of h for a given raise in contact pressure declined as P_c was increased; for example, the interface conductance at $P_c = 5$ MPa is 1.5 times greater than at 0.13 MPa. However, as P_c was raised from 5 to 10 MPa, this ratio in h decreases to just 1.2.

The magnitude of the interface conductance for the 0.28-μm rough surface was generally found to decrease as the heat flux was raised. In 760 Torr of helium, the decline in h was minimal and occurred almost entirely for $q < 100$ kW/m^2 (Fig. 23). In vacuum, however, the decrease in h was far more substantial and typically occurred over the entire range of heat fluxes (Fig. 24). It is surmised that this inverse relation between the magnitude of h and q is a result of macroscopic gap formation within the test interface due to nonuniform thermal deformation of the test specimens. In 760 Torr of helium, the gas layer appears to moderate the value of h such that gap formation has only a minimal impact on the interface conductance. In vacuum, however, the only heat transfer is via the interfacial contact area between the beryllium and steel surfaces. Thus, as q was increased and larger interstitial gaps formed, it was expected that the contact area, and therefore the interface conductance, would decrease. The experimental results for the 0.28-μm specimen tended to confirm this hypothesis.

The magnitude of h for the 6.25 μm surface, in 760 Torr of helium, was generally found to increase in value as the heat flux was raised (Fig. 25). The results were contrary to the results observed for the 0.28-μm surface, but were consistent with those results reported by Salerno and Kittel,[15] Van Sciver et al.,[16] and Schaellig and Seidel[17] for interfaces composed of similar materials. An explanation for this may be as follows: Increasing the heat flux was known to raise the mean interface temperature as well as the temperature of the steel specimen and the interstitial gas.[3] Because the interface conductance is proportional to thermal conductivity, and the thermal conductivity of helium, air, and steel increases with temperature (and heat flux),[3] one might expect that raising q would increase the magnitude of h, were it not for the deleterious effects of interstitial gap formation.

The present results may indicate that the taller surface asperities of the 6.25-μm surface acted as a compliant layer, actively filling any gaps that might form within the interface due to nonuniform thermal expansion. It is known from the literature that the yield strength

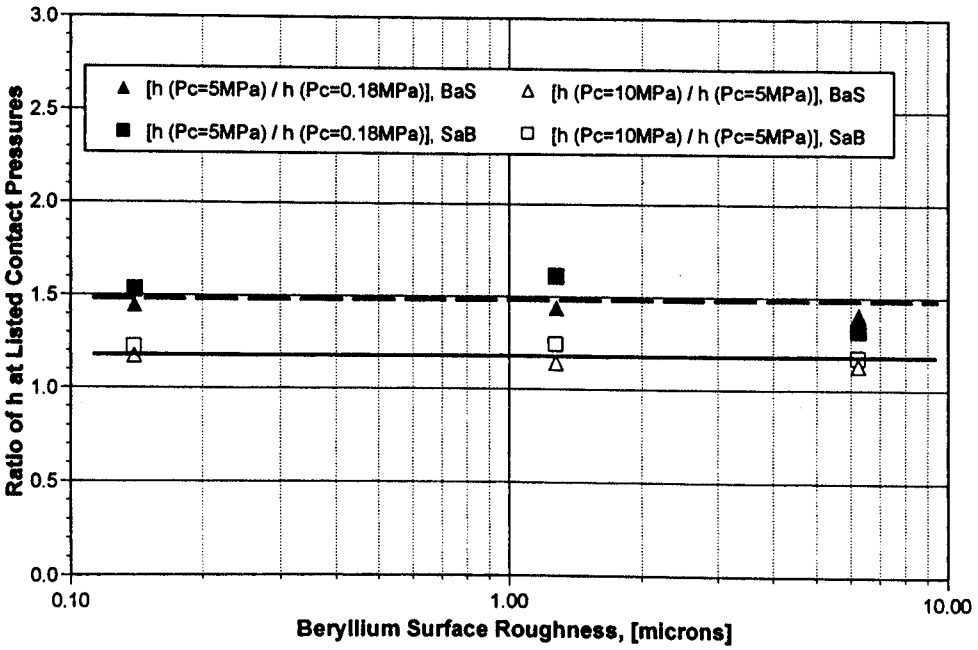

Fig. 22. Ratio of interface conductance versus beryllium surface roughness, 760-Torr helium, 1-in. disks, SaB and BaS disk orientations.

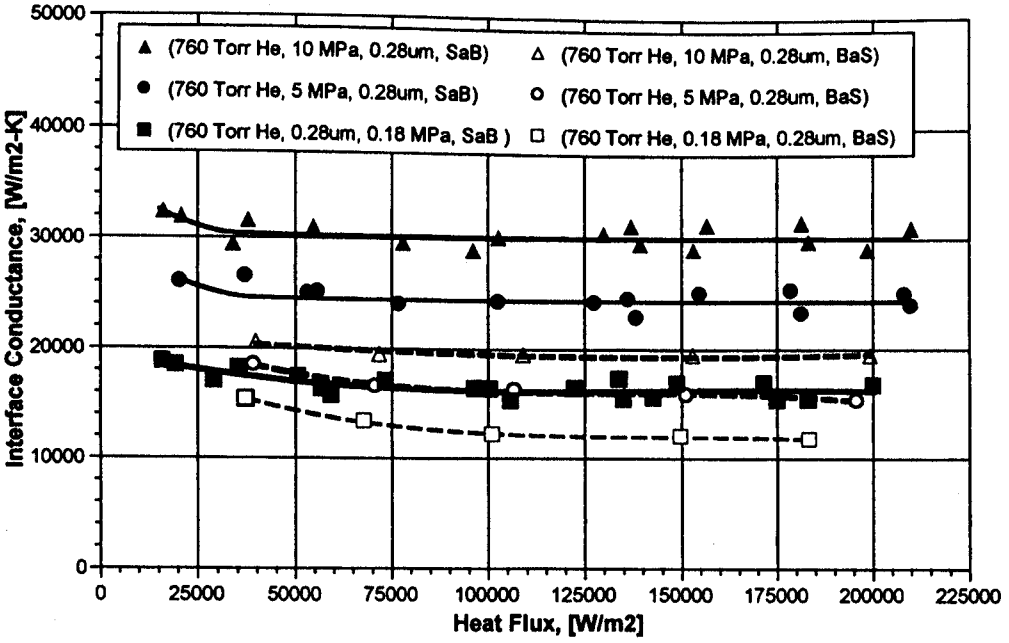

Fig. 23. Interface conductance versus heat flux, 760-Torr helium, 0.28-μm surface roughness, SaB and BaS configurations.

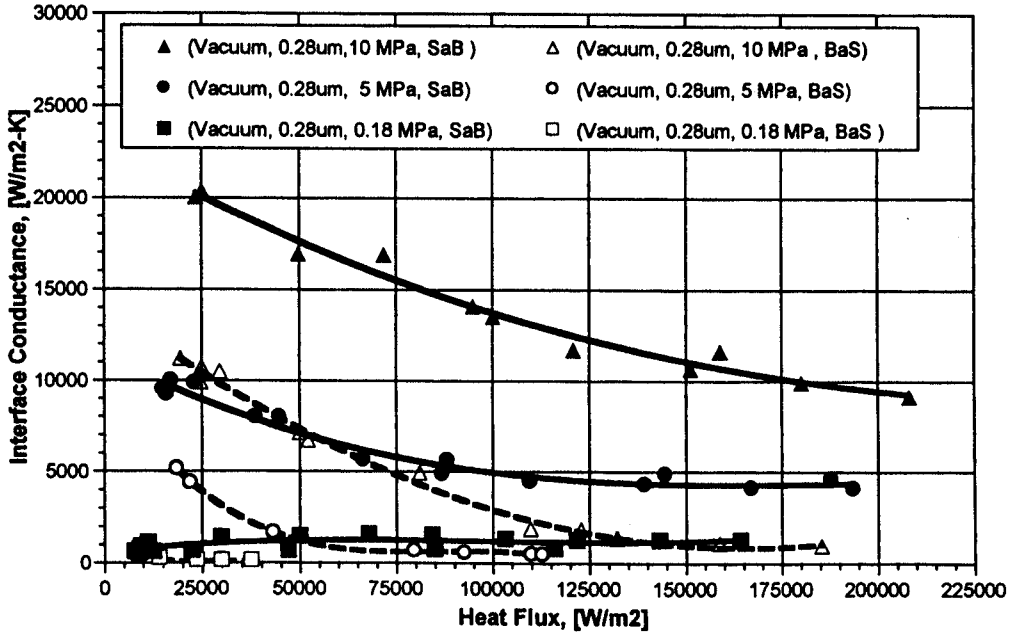

Fig. 24. Interface conductance versus heat flux, vacuum, 0.28-μm surface roughness, SaB and BaS configurations.

and Young's modulus of steel and beryllium is reduced as the temperature is increased. Therefore, increasing the heat flux would raise the temperature of the beryllium and steel specimens, resulting in the strength of their surface asperities being reduced. This could have led to a decrease in the mean separation distance (between the beryllium and steel surfaces), resulting in an increased value of interface conductance. Further research must be conducted to confirm these theories.

In summary, the interface conductance for 0.28- and 1.34-μm surfaces in vacuum was found to be very sensitive to heat flux, typically decreasing in magnitude as q was raised. For runs conducted in 760 Torr of helium, however, the value of h (for the same surfaces) appeared

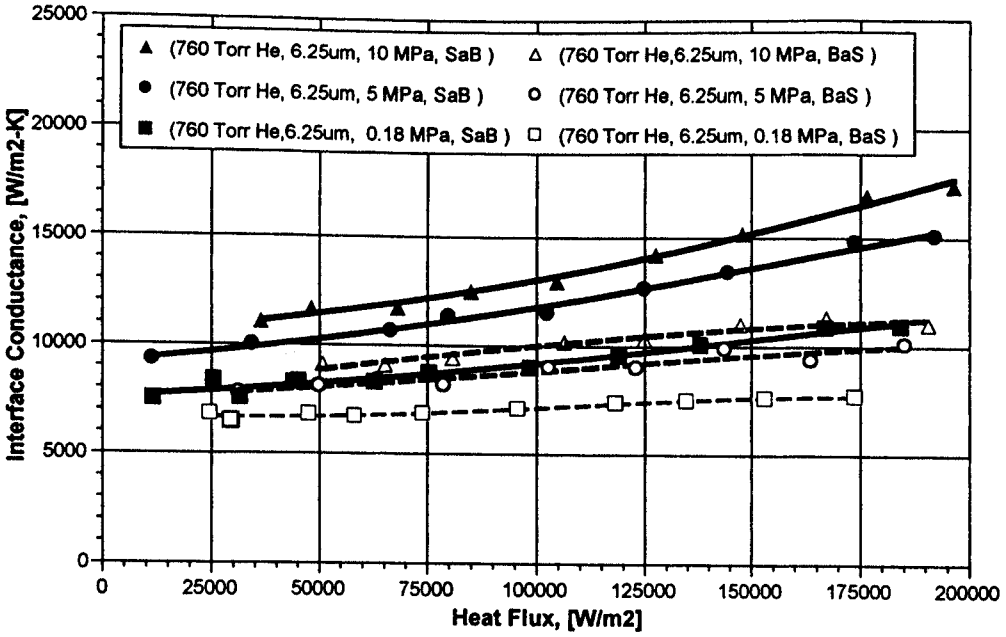

Fig. 25. Interface conductance versus heat flux, 760-Torr helium, 6.25-μm surface roughness, SaB and BaS configurations.

to be nearly independent of heat flux. The rougher 6.25-μm surface was found to be sensitive to heat flux both in vacuum and in 760 Torr of helium and generally saw h increase as the heat flux was raised up to ~175 kW/m^2, whereafter the interface conductance appeared to approach a steady value. The magnitude of h was found to be a function of the direction of the heat flux and was higher for disks in the SaB configuration. However, the gas conductance was found to be nearly independent of disk configuration, suggesting that it is the contact conductance component of h that is sensitive to the direction of heat flow. Finally, the presence of the interstitial gas made the relative increase in h for a given raise in contact pressure insensitive to the surface characteristics of the test specimens (surface roughness and disk orientation).

VI. INTERFACE CONDUCTANCE ERROR ANALYSIS

VI.A. Foreword

Eleven major contributors to the total uncertainty in h were considered in this analysis. These 11 error sources, and their respective magnitudes, are presented as follows (refer to Fig. 26 for error source location):

1. the calibration uncertainties of the four thermocouples installed within the beryllium and Type 316 stainless steel specimens, $\delta T_1 = \delta T_2 = \pm 0.13$°C, and in the aluminum heat flux meter, $\delta T_3 = \delta T_4 = \pm 0.13$°C.
2. the distance between the beryllium-Type 316 stainless steel interface and the thermocouple within the beryllium specimen, $\delta L_1 = \pm 0.1$ mm
3. the distance between the beryllium-Type 316 stainless steel interface and the thermocouple within the Type 316 stainless steel steel specimen, $\delta L_2 = \pm 0.1$ mm
4. the distance between the two thermocouples installed in the heat flux meter, which are used to calculate the magnitude of the heat flux, $\delta L_3 = \pm 0.1$ mm
5. the thermal conductivity of the beryllium specimen, $\delta k_{Be} = \pm 10\%$
6. the thermal conductivity of the Type 316 stainless steel specimen, $\delta k_{SS316} = \pm 3\%$
7. the thermal conductivity of the aluminum heat flux meter material, $\delta k_{Al} = \pm 3\%$
8. the radiative and convective heat losses from the experimental test apparatus, referred to as Leakage.

There are several established methods that may be employed to perform an uncertainty analysis. The most common procedure is that given by Moffat[18] and the *Journal of Heat Transfer*[19] and involves treating every identifiable error source (i.e., temperature measurements, lengths between thermocouples, thermal conductivities, etc.) as a random error. In doing this, it is assumed that each individual error will change from run to run following a Gaussian distribution. For later reference, this

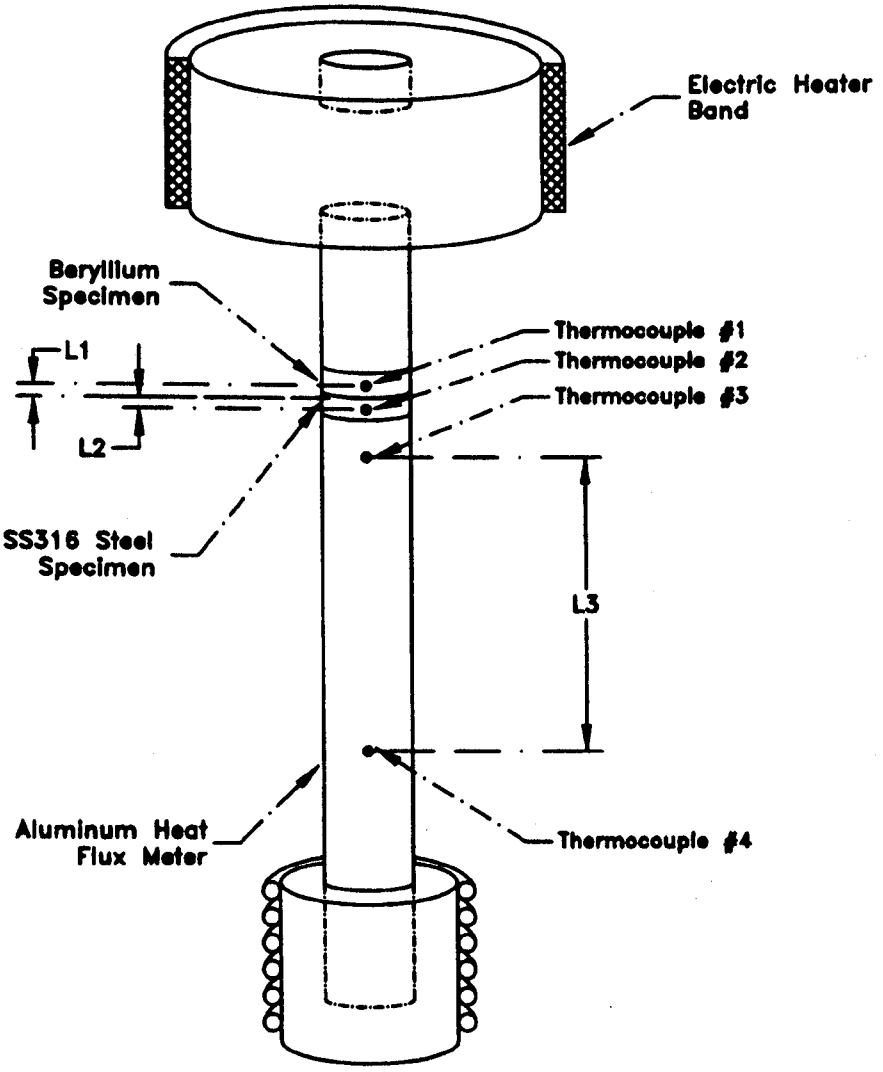

Fig. 26. General diagram of the interface heat conductance test apparatus, BaS configuration.

methodology will be referred to as the TER method. Following the TER methodology, the total expected error in interface conductance, denoted as δh, is given by the following root sum square relation:

$$\delta h = [(\delta h|_{\delta T_1})^2 + (\delta h|_{\delta T_2})^2 + (\delta h|_{\delta T_3})^2 + (\delta h|_{\delta T_4})^2 + (\delta h|_{\delta L_1})^2 + (\delta h|_{\delta L_2})^2 + (\delta h|_{\delta L_3})^2 + (\delta h|_{\delta k_{Be}})^2 + (\delta h|_{\delta k_{SS316}})^2 + (\delta h|_{\delta k_{Al}})^2 + (\delta h|_{Leakage})^2]^{1/2} \quad . \qquad (6)$$

In this relation, $\delta h|_{\delta T_i}$ is the uncertainty in h due solely to temperature measurement error δT_i (where T_i is any one of the four thermocouples employed in the rig) and $\delta h|_{\delta L_j}$ is the uncertainty in h due solely to length measurement error δL_j (where L_j is any one of the three critical lengths listed in Fig. 26) . Additionally, $\delta h|_{\delta k_m}$ is the uncertainty in h due solely to thermal conductivity error δk_m (where k_m is either the thermal conductivity of beryllium, Type 316 stainless steel, or aluminum) and $\delta h|_{Leakage}$ is the error in interface conductance due to both convective and radiative heat losses.

The problem with using the TER procedure is that not every error source changes from run to run. For example, the thermal conductivities of the Type 316 stainless steel specimen and the aluminum heat flux meter were measured and curve fitted before any interface conductance measurements were made. We do not remeasure k_{SS316} and k_{Al} between every interface conductance measurement, and thus, the uncertainties in k_{SS316} and k_{Al} clearly act as bias errors in the calculation of h. The result of assuming these two error sources behave in a random manner is to severely underpredict the true magnitude of δh.

The second method for performing a sensitivity analysis is that outlined by Mills[20] and Taylor[21] and will be referred to here as the DBRE method. In following this procedure, random error sources (e.g., temperature measurements) and bias error sources (e.g., lengths between thermocouples, measured thermal conductivities, and radiative and convective heat losses) are treated as two distinct entities. The total uncertainty error in h is then given by the following expression:

$$\delta h = \pm \delta h_{random} \pm \delta h_{bias} \ , \tag{7}$$

where the random and bias error components are defined by

$$\delta h_{random} \equiv \sqrt{(\delta h|_{\delta T_1})^2 + (\delta h|_{\delta T_2})^2 + (\delta h|_{\delta T_3})^2 + (\delta h|_{\delta T_4})^2} \tag{8}$$

and

$$\delta h_{Bias} \equiv \pm \delta h|_{\delta L_1} \pm \delta h|_{\delta L_2} \pm \delta h|_{\delta L_3} \pm \delta h|_{\delta k_{Be}} \pm \delta h|_{\delta k_{Al}} \pm \delta h|_{\delta k_{SS316}} \pm \delta h|_{Leakage} \ . \tag{9}$$

The advantage of this method is that it treats random and bias errors distinctly and correctly, resulting in a more accurate sensitivity analysis. The disadvantage is that it tends to give a worst-case error estimate, which may be overly conservative. As previously mentioned, the difference between errors estimated by using this procedure versus the TER procedure (where all errors are treated as random errors) can be significant.

Because both of the aforementioned methods are useful indicators of how accurate a given interface conductance measurement is, error bars were generated using both the TER and DBRE methodologies for a select number of interface conductance data.

VI.B. Uncertainty Estimates for h versus P_c Measurements

The uncertainty error in h has been calculated over a range of surface roughnesses, contact pressures, gas pressures, and gas types to give an idea how δh varies with respect to these parameters. Both the TER and the DBRE methodologies were used to compute the uncertainty errors and generate error bars in the following figures.

In addition to the 11 error sources previously discussed, there are 3 additional sources of uncertainty that should be mentioned. The first is the error in the independent variable P_c. Because of load cell calibration errors and the imprecise nature of controlling the contact pressure with a hand-operated hydraulic press, the magnitude of the external loading is only good to ± 10 pounds, which corresponds to 1-in.-diam specimens. Clearly, on a scale that ranges from 0.18 to 12 MPa, the uncertainty in P_c is negligible and does not warrant adding horizontal error bars to any of the figures.

The magnitude of the gas pressure is another source of error in two different capacities:

1. in the reading of the pressure via the Convectron and Baratron transducers
2. in regulating the gas pressure via the proportional control valve and feedback loop.

The transducers had a typical measurement uncertainty of <5%, while the pressure regulation system was able to hold P_g to within 5% of the selected value. The effect of these uncertainties on the magnitude of h was observed to be minimal relative to all other error sources, and thus, they were not included in any of the error bars.

Finally, it was expected that plastic deformation of the surface asperities would result in large discrepancies between repeated results. This was not found to be the case. Some surface deformation was visible in the form of a smooth annular ring when the specimens were in the SaB configuration, and a concentric circle for runs carried out in the BaS configuration. However, repeated measurements failed to indicate any notable change in h that could be definitely attributed to surface smoothening.

Figures 27 and 28 present uncertainty estimates for the 6.25-μm rough surfaces as a function of contact pressure using the TER and DBRE methodologies, respectively. Error bars are presented for runs carried out in vacuum, in 760 Torr of air and in 760 Torr of helium, and selected numerical values are listed in Table II. In general, the magnitude of the measurement error was minimized when the temperature difference across the beryllium-steel interface was large. Thus, the most accurate h readings were obtained in vacuum and at low contact pressures. The magnitudes of the DBRE error estimates were often twice those of the associated TER estimates. This indicated that the test rig was dominated by bias error sources (lengths, thermal conductivities, and convection heat losses) rather than by random error sources (thermocouple temperature measurements). The three dominant error sources were the uncertainties in Type 316 stainless steel thermal conductivity, aluminum thermal conductivity and the distance between the test interface and the thermocouple within the Type 316 stainless steel specimen (Fig. 26).

The uncertainty errors for h measurements made with the lapped beryllium surface (combined beryllium-Type 316 stainless steel disk roughness = 0.28 μm) are presented in Figs. 29 and 30 using the TER and DBRE methodologies. Selected numerical values are listed in Table III. The magnitude of the interface conductance was typically very high (as great as 35 000 W/m^2·K) for runs carried out in 760 Torr of gas, resulting in a very small interfacial temperature drop (on the order of 5°C). This small temperature difference greatly increased the uncertainty in the h measurements due to the 11 error

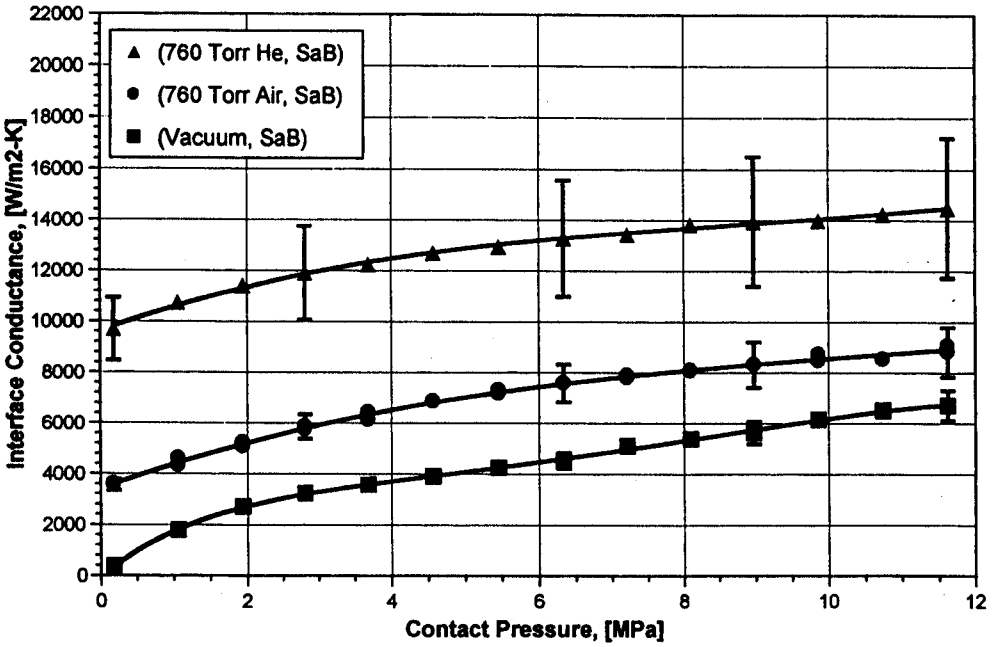

Fig. 27. Measurement uncertainty for h versus P_c, using TER methodology, 6.25-μm disks, in 760-Torr (air and helium) and in vacuum, SaB configuration.

sources previously mentioned (the uncertainty in h could be as great as 99%). However, a high value of interface conductance means the interfacial resistance is very small and, therefore, generally unimportant for most practical applications. Thus, the large uncertainties encountered under 760 Torr of gas do not invalidate the usefulness of the data; rather, the associated large values of h indicate that the interfacial resistance may be of negligible

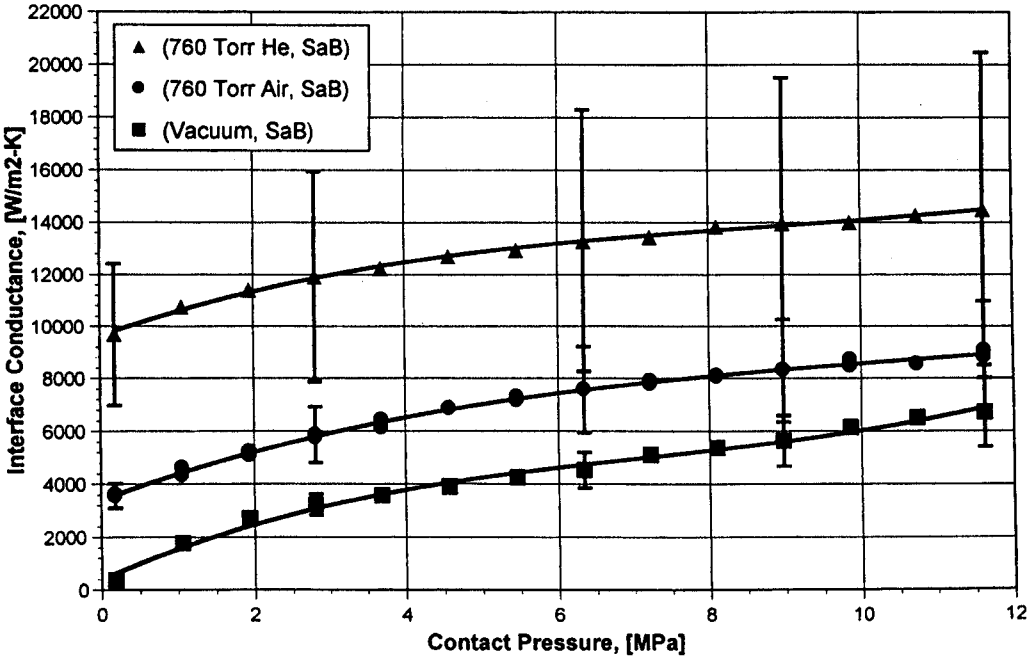

Fig. 28. Measurement uncertainty for h versus P_c, using DBRE methodology, 6.25-μm disks, in 760-Torr (air and helium) and in vacuum, SaB configuration.

TABLE II

Measurement Error in h for the 6.25-μm Surface at Selected Values of Contact Pressures, Gas Pressure, and Gas Type

Contact Pressure (MPa)	Gas Pressure/Type	TER Error in h (%)	DBRE Error in h (%)
0.18	Vacuum	4.4	7.1
6.38	Vacuum	6.9	15
11.6	Vacuum	8.8	19
0.18	760 Torr/air	6.3	13
6.38	760 Torr/air	9.8	22
11.6	760 Torr/air	11	24
0.18	760 Torr/helium	13	28
6.38	760 Torr/helium	17	38
11.6	760 Torr/helium	18	41

importance when lapped surfaces are used in 760 Torr of gas under high contact pressures.

VI.C. Uncertainty Estimates for h versus q Measurements

The measurement uncertainty h was computed as a function of heat flux for runs carried out under 5 MPa of contact pressure, with disks of 6.25, 1.34, and 0.28 μm of surface roughness. Selected numerical results are presented in Table IV for measurements made in vacuum, and the associated error bars are displayed in Fig. 31 (TER methodology) and Fig. 32 (DBRE methodology). The analogous TER and DBRE error bars for runs carried out in 760 Torr of helium are presented in Figs. 33 and 34.

From Table IV, observe that the magnitude of the error in h is inversely related to the magnitude of the heat flux. When measurements were made at low values of q, the temperature difference across the test interface would often be very small (typically on the order of 1 to 5°C), making it difficult to accurately compute the magnitude of h [using Eq. (5)]. Typically, the measurement uncertainty of the four thermocouples would dominate the error in h as the magnitude of the heat flux was reduced below 50 kW/m^2.

The uncertainty in the interface conductance measurements was generally observed to increase along with the magnitude of h. Thus, the error bars were larger for smoother surfaces than for rougher surfaces (Figs. 31 and 32) and for measurements made in 760 Torr of helium as opposed to vacuum (Figs. 33 and 34). The relationship between the magnitude of h and the uncertainty in h is as follows: A higher value of interface conductance implies a smaller interfacial temperature difference ΔT_i for a fixed value of heat flux [Eq. (5)]. At lower values of h (i.e., in vacuum, using rough surfaces, etc.), the magnitude of ΔT_i is typically large (an order of tens of degrees Celsius), and its value was not greatly affected by uncertainties in temperature measurements ($\delta T = \pm 0.13$°C), length

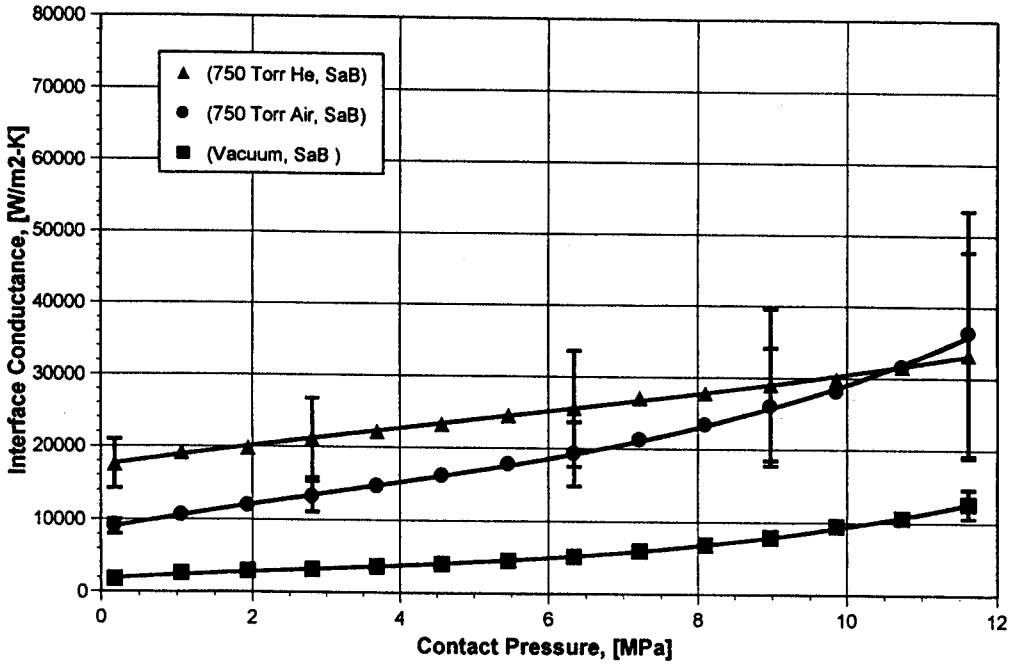

Fig. 29. Measurement uncertainty for h versus P_c, using TER methodology, 0.28-μm disks, in 760-Torr (air and helium) and in vacuum, SaB configuration.

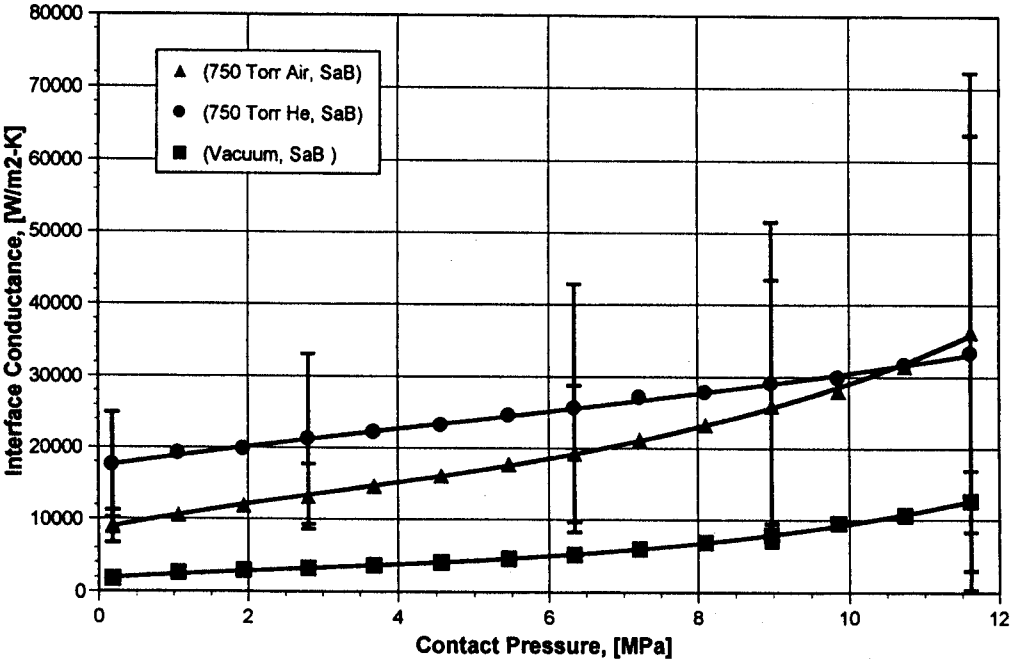

Fig. 30. Measurement uncertainty for h versus P_c, using DBRE methodology, 0.28-μm disks, in 760-Torr (air and helium) and in vacuum, SaB configuration.

measurements, etc. However, as the interface conductance was increased, the magnitude of ΔT_i could be reduced to the order of just 1°C. This made the values of the uncertainties (in temperature, length, etc.) nearly the same magnitude as h, resulting in a large relative error in the interface conductance measurement.

For h versus q runs carried out in 760 Torr of helium, the temperature difference across the test interface was typically many times smaller than for runs carried out in vacuum, resulting in interface conductance measurement errors that were substantially higher when compared with runs carried out in vacuum. Numerical values of the TER and DBRE errors are listed in Table V for a selected range of heat fluxes, and the associated error bars are presented in Figs. 33 and 34.

Following the TER methodology, the average uncertainty in h was ~16, 22, and 35% for surface roughnesses of 6.25, 1.34, and 0.28 μm, respectively. Because

TABLE III

Measurement Error in h for the 0.28-μm Surface at Selected Values of Contact Pressures, Gas Pressure, and Gas Type

Contact Pressure (MPa)	Gas Pressure/ Gas Type	TER Error in h (%)	DBRE Error in h (%)
0.18	Vacuum	4.8	8.6
6.38	Vacuum	7.3	16
11.6	Vacuum	15	33
0.18	760 Torr/air	11	25
6.38	760 Torr/air	23	49
11.6	760 Torr/air	47	99
0.18	760 Torr/helium	20	44
6.38	760 Torr/helium	32	68
11.6	760 Torr/helium	43	91

TABLE IV

Uncertainty in h in Vacuum at Selected Values of Heat Flux, P_c = 5 MPa, All Roughnesses

Heat Flux ($W/m^2 \cdot K$)	Be Surface Roughness (μm)	TER Error in h (%)	DBRE Error in h (%)
22 140	6.25	6.0	13
96 090	6.25	6.0	13
183 850	6.25	6.5	14
26 210	1.34	18	39
96 930	1.34	14	32
190 140	1.34	4	8.4
17 130	0.28	19	41
109 660	0.28	7.0	16
193 570	0.28	6.6	14

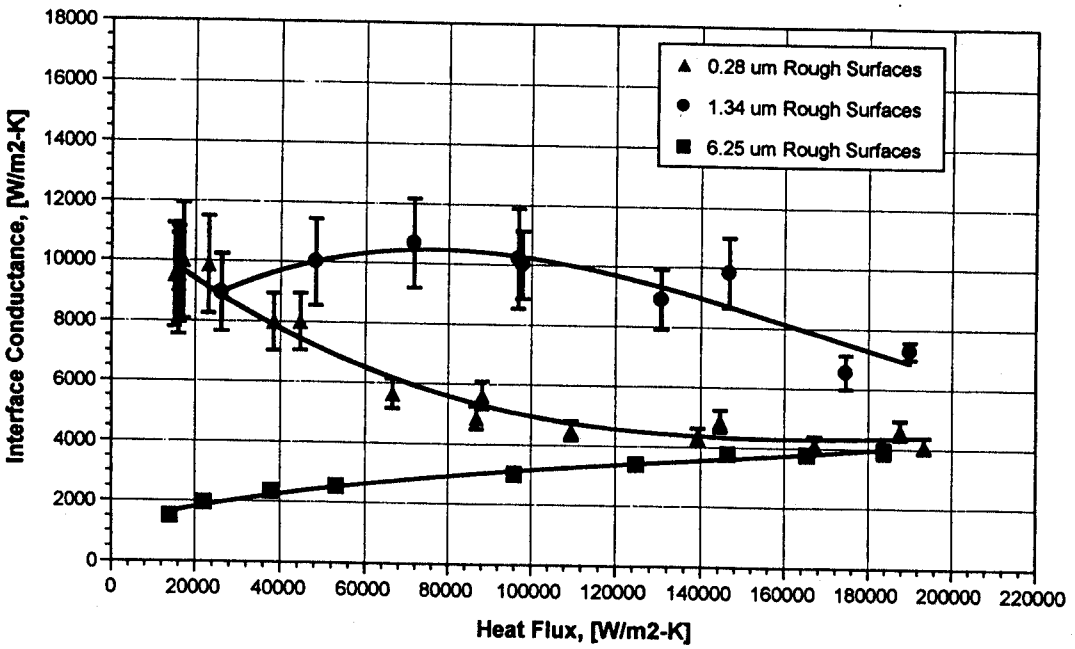

Fig. 31. Measurement uncertainty for h versus q, using TER methodology, $P_c = 5$ MPa, vacuum, SaB configuration.

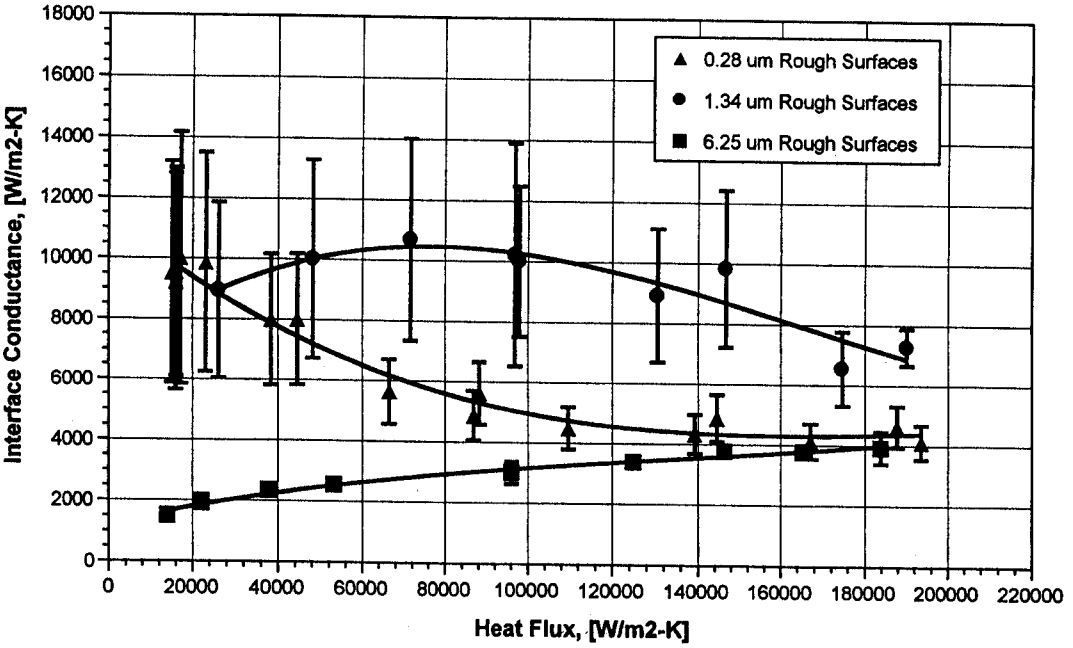

Fig. 32. Measurement uncertainty for h versus q, using DBRE methodology, $P_c = 5$ MPa, vacuum, SaB configuration.

of their lower values of interface conductance, rougher surfaces could be more accurately characterized than smoother surfaces. The magnitude of the DBRE error estimates are roughly twice those of the TER estimates, with the uncertainty dominated by errors in the thermal conductivity of Type 316 stainless steel and aluminum, and by the measured distance between the test interface and the thermocouple installed in the steel test specimen.

VII. SUMMARY

Interface heat conductance was measured between roughened beryllium and lapped stainless steel as a function of numerous geometric, surface, and environmental parameters. The value of the interface conductance was within the order of magnitude range of 100 to 100 000 $W/m^2 \cdot K$, which is consistent with similar

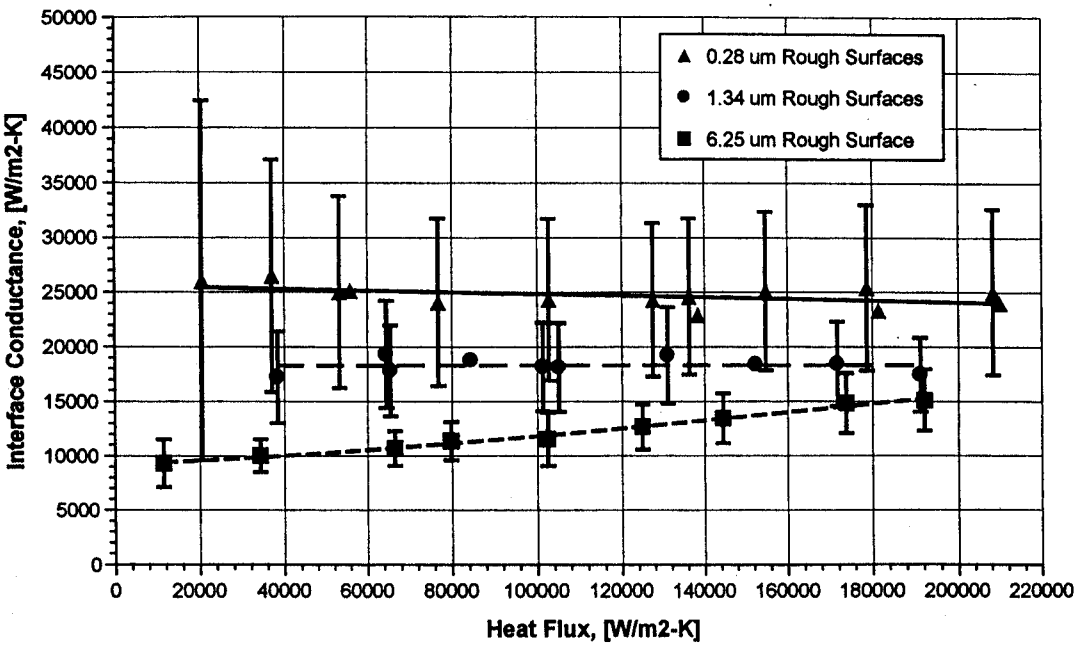

Fig. 33. Measurement uncertainty for h versus q, using TER methodology, P_c = 5 MPa, 760-Torr helium, SaB configuration.

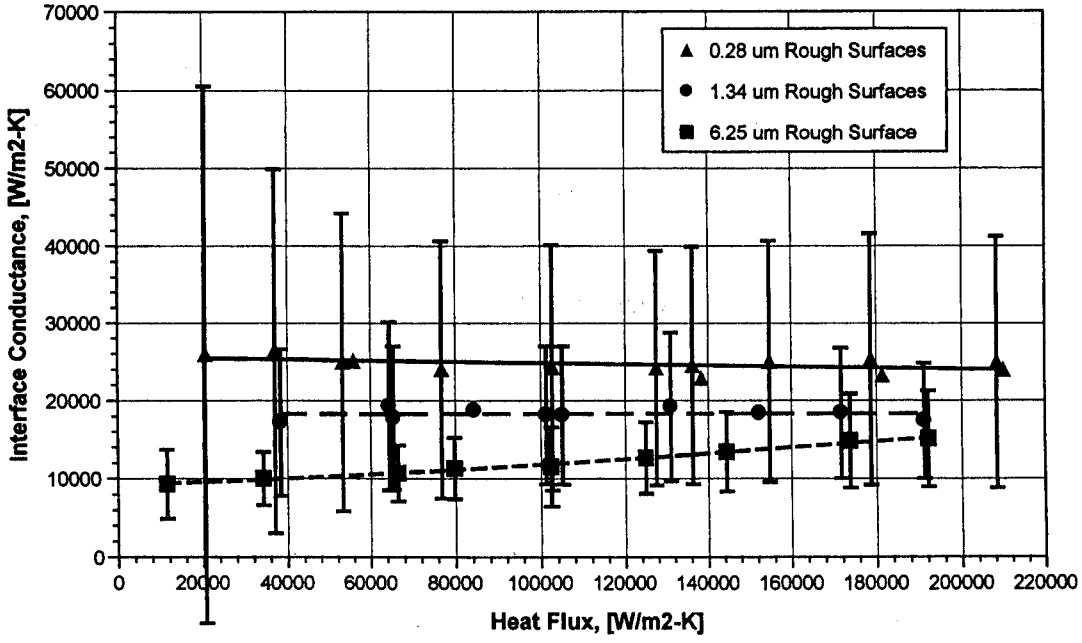

Fig. 34. Measurement uncertainty for h versus q, using DBRE methodology, P_c = 5 MPa, 760-Torr helium, SaB configuration.

metal-metal contacts reported in the literature (e.g., Van Sciver et al.[16]).

Lapped surfaces possessed values of h as great as 80 000 $W/m^2 \cdot K$ under high contact pressures and in 760 Torr of gas. The magnitude of the interface conductance for these smooth surfaces, however, was very sensitive to contact pressure, gas pressure, and heat flux. Because the associated interfacial resistance under these conditions was very low (and therefore unimportant for most practical applications), the variation of h with respect to the foregoing parameters may not be a significant concern.

Rougher (e.g., ball-bearing-blasted and sand-blasted) surfaces were found to have much lower values of

NOMENCLATURE

h = interface conductance ($W/m^2 \cdot K$)

h_c = control conductance

h_g = gas conductance

k_{Be}, k_{Steel}, k_{Al} = thermal conductivity of beryllium, stainless steel, and aluminum ($W/m \cdot K$)

k_1, k_2 = conductivity of the contacting solids ($W/m \cdot K$)

L_{i-2} = distance between thermocouple 2 and interfacing surface

L_{1-i} = distance between thermocouple 1 and interfacing surface

L_{3-4} = distance between 2 thermocouples in cylindrical Al Rod

P_c = contact pressure (mPa)

P_g = gas pressure (Torr or mTorr)

Q = applied heater power (W)

q = heat flux (W/m^2)

T_i^{Be} = extrapolated temperature, beryllium interfacing surface

T_i^{steel} = extrapolated temperature, steel interfacing surface

T_s = temperature at the mathematical s-surface

T_u = temperature at the mathematical u-surface

T_1 = temperature of Be at location 9, thermocouple 1

T_2 = temperature of steel at location 9, thermocouple 2

Greek

ΔT_i = temperature difference across the interface

δh = total uncertainty in the value of h ($W/m^2 \cdot K$)

δh_{Bias} = uncertainty in the value of h due to bias errors ($W/m^2 \cdot K$)

δh_{Random} = uncertainty in the value of h due to random errors ($W/m^2 \cdot K$)

REFERENCES

1. A. F. MILLS, *Heat Transfer*, Irwin Publishing, Homewood, Illinois (1992).

2. G. E. SHATALOV et al., "Breeder and Test Blankets in ITER," *Fusion Eng. Des.*, **16**, 85 (1991).

3. R. D. ABELSON, "Experimental Measurement and Analytical Modeling of the Interface Heat Conductance Between Non-Conforming Beryllium and SS316 Surfaces Subjected to Non-Uniform Thermal Deformations," PhD Thesis, University of California, Los Angeles, Department of Mechanical and Aerospace Engineering (1999).

4. D. E. DOMBROWSKI, E. DEKSNIS, and M. A. PICK, "Thermomechanical Properties of Beryllium," TR-1182, *Atomic and Plasma Interaction Data for Fusion*, Vol. 5, p. 15, International Atomic Energy Agency (1995).

5. R. D. ABELSON and M. A. ABDOU, "Experimental Evaluation of the Interface Heat Conductance Between Roughened Beryllium and Stainless Steel Surfaces," *J. Nucl. Mater.*, **233–237**, 847 (1996).

6. R. D. ABELSON, "Analytical and Experimental Measurements of Interface Conductance Between Roughened Beryllium and Steel Surfaces," MS Thesis, University of California, Los Angeles, Department of Mechanical and Aerospace Engineering (1995).

7. R. BERMAN, "Some Experiments on Thermal Contact at Low Temperatures," *J. Appl. Phys.*, **27**, *4*, 318 (Apr. 1956).

8. C. STARR, "The Copper Oxide Rectifier," *J. Appl. Phys.*, **7**, 15 (1936).

9. M. E. BARZELAY, K. N. TONG, and G. F. HOLLOWAY, "Effect of Pressure on the Thermal Conductance of Contact Points," NACA, Technical Note 3295, National Advisory Committee for Aeronautics (1955).

10. G. F. C. ROGERS, "Heat Transfer at the Interface of Dissimilar Metals," *Int. J. Heat Mass Transfer*, **2**, 150 (1961).

11. S. WILLIAMS, "An Investigation into the Possible Rectification of Heat Flow Across Dissimilar Metal Contacts," PhD Thesis, Manchester University, England (1966).

12. A. M. CLAUSING, "Heat Transfer at the Interface of Dissimilar Metals—The Influence of Thermal Strain," *Int. J. Heat Mass Transfer*, **9**, 791 (1966).

13. D. V. KEWIS and H. C. PERKINS, "Heat Transfer at the Interface of Stainless Steel and Aluminum—The Influence of Surface Conditions on the Directional Effect," *Int. J. Heat Mass Transfer*, **11**, 1371 (1968).

14. T. R. THOMAS and S. D. PROBERT, "Thermal Contact Resistance: The Directional Effect and Other Problems," *Int. J. Heat Mass Transfer*, **13**, 789 (1969).

15. L. J. SALERNO and P. KITTEL, "Thermal Contact Conductance," *Handbook of Cryogenic Engineering*, p. 165, Taylor and Francis, Philadelphia, Pennsylvania (1998).

16. S. W. VAN SCIVER, M. J. NILLES, and J. PFOTENHAUER, "Thermal and Electrical Contact Conductance Between Metals at Low Temperatures," Space Cryogenic Workshop Papers, University of Berlin, Berlin, Germany, August 1980, p. 37.

17. R. SCHAELLIG and A. SEIDEL, "Very Low Force Cooling Contact for the ISO Cryostat Cover," *Cryogenics*, **30**, 173 (Mar. 1990).

18. R. J. MOFFAT, "Describing the Uncertainties in Experimental Results," *Experimental Thermal and Fluid Science*, Vol. 1, p. 3, Elsevier, New York (1988).

19. "Journal of Heat Transfer Policy on Reporting Uncertainties in Experimental Measurements and Results," *J. Heat Transfer*, **115**, 5 (1993).

20. A. MILLS, "Error Assessment: M157 Lab Manual," Mechanical and Aerospace Engineering Department, University of California, Los Angeles (1992).

21. J. R. TAYLOR, "An Introduction to Error Analysis," Oxford University Press, New York (1982).

Robert Dean Abelson [PhD, University of California, Los Angeles (UCLA), 1999] is currently the manager of one of Boeing's Engineering Support Rooms for the International Space Station (ISS) program. In this capacity, he coordinates ISS mission operations with his team of more than 200 space station engineers. He also prepares Boeing and U.S. National Aeronautics and Space Administration personnel for ISS mission operations by developing and presenting training courses in the conduct of mission support. His previous research work was in the field of interface heat conductance between nonconforming beryllium and steel surfaces.

Mohamed A. Abdou (PhD, University of Wisconsin, 1973) is a professor in the Mechanical and Aerospace Engineering Department. He is also the director of the Fusion Science and Technology Center at UCLA. His research interests cover engineering sciences and technology for advanced energy systems, including fusion reactor design and analysis, material system thermomechanics, fluid flow, neutronics, and high heat flux technology.